TRI-PP-89-25
May 1989

A Dynamical Model of Pion Photoproduction on the Nucleon

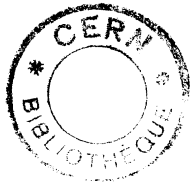

S. Nozawa
TRIUMF, 4004 Wesbrook Mall, Vancouver B.C., Canada V6T 2A3
and Paul Scherrer Institute, CH-5232 Villigen PSI, Switzerland

B. Blankleider
Paul Scherrer Institute, CH-5232 Villigen PSI, Switzerland

T.-S. H. Lee
Argonne National Laboratory, Argonne, Illinois, U.S.A.

(Submitted to *Phys. Rev. C.*)

ABSTRACT

Pion photoproduction on the nucleon is investigated using a model Hamiltonian defined in the channel-space $\mathcal{H} = \pi N \oplus \pi\gamma \oplus B$ with $B = \Delta$ and N. The basic electromagnetic matrix elements are deduced from the low-order Feynman amplitudes calculated from a Lagrangian describing interactions among $\gamma, \pi, \rho, \omega, N$ and Δ fields. The πN interaction is described by $B \leftrightarrow \pi N$ vertices, and a two-body separable potential. A scattering formalism is introduced to assure that the constructed pion photoproduction amplitude is unitary and gauge invariant. The πN parameters are determined by fitting the phase shift data up to 500 MeV incident pion energy. The remaining three free parameters of the model, cutoff Λ for the form factor which regularizes the Born (non-resonant) terms, G_M and G_E for the $\gamma N \leftrightarrow \Delta$ vertex, are determined by fitting the $M_{1+}(3/2)$ and $E_{1+}(3/2)$ multipole data. The resulting $E2/M1$ ratio of the $\gamma N \leftrightarrow \Delta$ excitation is -3.1%. The model provides a good description of the existing cross section and polarization data for $\gamma p \to \pi^+ n$, $\gamma p \to \pi^0 p$ and $\gamma n \to \pi^- p$ up to 500 MeV incident photon energy. The importance of unitary in extracting the basic parameters from the data is demonstrated explicitly. It is also shown, that within the present unitary model, the πN off-shell effects can account for up to 50% of the cross section. This calls into question those models that only use Watson's theorem to impose unitarity. The model is consistent with the existing unitary πNN models, and hence can be directly applied to study pion photoproduction on the deuteron and heavier nuclei.

I. Introduction

The electromagnetic production of pions on the nucleon has long been studied since the publication of the pioneering work by Chew, Goldberger, Low and Nambu (CGLN).[1] Extensive work during these more than thirty years[2-17] indicates that, below 500 MeV incident photon energy, the dominant mechanisms of the $\gamma N \to \pi N$ reaction are the Born term (arising from minimal substitution in the πN Lagrangian) and the Δ excitation, as illustrated in Fig. 1. At the same time, and quite separately, much progress has been made at describing purely hadronic systems. Here the strong interactions make it less appropriate to use lowest order contributions. Thus the emphasis has been on a careful treatment of multiple scattering, and therefore unitarity. A prime example of such an approach is given by the unitary models of the πNN system.[18-22] Until very recently, little attention has been given to extending these multiple scattering formulations to include coupling to electromagnetic interactions. In this paper we present a calculation of $\gamma N \to \pi N$ that incorporates πN multiple scattering, and therefore forms a first step at combining these two traditionally different areas of nuclear physics. Starting with these well-studied models, we will construct a dynamical model which has the following features: (1) It is unitary and gauge invariant, (2) It can describe most of the existing $\gamma N \leftrightarrow \pi N$ data below 500 MeV incident photon energy, (3) It relates the electromagnetic excitation of the Δ resonance to the chiral/cloudy bag model[23] of hadron structure, (4) It can be straightforwardly included in the current πNN models[18-22] for investigating intermediate energy electromagnetic interactions with two- and many-nucleon systems. The paper will give a detailed presentation of how (1)-(3) are achieved. Although (4) will be established theoretically, its numerical consequences will not be discussed here.

In order to see the main features of the present approach, it is necessary to briefly review the previous theoretical studies. Basically there exist three main approaches. The first one is the extension of the CGLN model based on the dispersion-relation formulation. It makes use of the properties of unitarity, analyticity and crossing symmetry to express the photoproduction amplitudes in terms of πN scattering amplitudes and the Born terms calculated from a Lagrangian. The development peaked in 1967 with the publication of three papers by Berends, Donnachie and Weaver.[2] In general the dispersion-relation approach can account for the main features of the data. Its main difficulty is to describe π^- production data above the Δ-region. The results of Ref. 2 and earlier works were reviewed by Donnachie.[3]

The second approach is the effective Lagrangian method which utilizes Chiral symmetry. By gauging a Chiral Lagrangian[4] to include coupling to the electromagnetic field, the pion photoproduction mechanism is calculated with perturba-

tion theory in the tree-approximation (only keeping the terms without loop integrations). The final πN interaction is accounted for by using Watson's theorem.[24] This requires that the phase of each photoproduction multipole amplitude is identical to the πN scattering phase in the same eigenchannel. This approach was thoroughly investigated by Olsson and Osypowski.[5] They emphasized that the pion photoproduction mechanism should be calculated with pseudovector coupling, as required by Chiral symmetry. They also found that a satisfactory agreement with data can only be achieved when the exchange of vector mesons, and an explicit treatment of the Δ degree of freedom are included. Their approach was further developed by Wittman, Mukhopadhyay and Davidson,[6] as well as by Sabutis.[7] The model developed by Blomqvist and Laget[8,9] can be considered as a variation of the effective Lagrangian approach.

Here it is necessary to point out, that in these two approaches the final πN interaction is described only by the πN scattering phase shifts. Within their theoretical frameworks, no procedure is defined to calculate the off-shell amplitudes which are indispensable in nuclear calculations. Clearly we have to go beyond these two approaches in order to obtain feature (4) stated in the beginning of this section.

We now turn to describe the third approach, which will be adopted in this work. This is a Hamiltonian formulation which is closely related to two recent developments in intermediate energy nuclear physics: (1) the construction of a nuclear Hamiltonian with π, N and Δ degrees of freedom - especially as arising in the extensive studies of the πNN system,[18-22] (2) the study of nucleon structure and πN scattering within the chiral/cloudy bag model.[23] It is assumed that the πN interaction Hamiltonian consists of a $\pi N \leftrightarrow \Delta$ vertex and a two-body πN potential. The electromagnetic parts of the Hamiltonian are defined in terms of matrix elements calculated from a Lagrangian using perturbation theory. In the simplest version, the vertex interactions of the Hamiltonian, such as $\pi N \leftrightarrow \Delta$ and $\gamma N \leftrightarrow \Delta$, can be parametrized with any convenient form. A more constraining approach would be to relate these vertices, at least qualitatively, to chiral bag model parameters. The first attempts to construct such a Hamiltonian model were made by Tanabe and Ohta,[10] who considered only the P_{33} channel, and independently by Yang,[11] who considered all s- and p-wave amplitudes. The model developed by Heller, Kumano, Martinez and Moniz[12] in their study of πN bremsstrahlung, is also based on the same theoretical considerations. It has been extended by Kumano[13] to investigate $\gamma N \leftrightarrow \Delta$ in the $p(e, e'\pi)$ reaction. A number of other closely related works have investigated the $\gamma N \leftrightarrow \Delta$ transition in the context of a chiral bag model.[14-16] The most ambitious approach is the one developed by Araki and Afnan.[17] They employed the diagrammatic method to derive a set of coupled $\gamma N - \pi N$ unitary equations from the cloudy bag Lagrangian. No numerical results based on their approach have been reported so far.

In this work we will present a Hamiltonian approach which accomplishes the four objectives listed in the beginning of this section. In many ways our approach is closely related to the works by Tanabe and Ohta[10] and Yang.[11] The advances accomplished in this work are: (1) A gauge invariant current operator is defined in terms of Feynman amplitudes with no non-relativistic reduction being necessary. Instead, a careful selection of intermediate state momenta enables an effective "three-dimensional reduction". (2) The same approach is also used to define the $\gamma N \leftrightarrow \Delta$ vertex function using the covariant form of Jones and Scadron[25] which describes the Δ as a Rarita-Schwinger field. (3) The P_{33} πN interaction is parametrized according to the cloudy bag model (other partial waves, up to d waves, are described by separable potentials). (4) Satisfactory agreement with existing cross section and polarization data is demonstrated for $\gamma p \to \pi^+ n$, $\gamma p \to \pi^0 p$ and $\gamma n \to \pi^- n$ reactions. (5) The role of the πN off-shell amplitudes in determining the cross sections and multipole amplitudes is explored in detail. This explicitly illustrates the differences between the Hamiltonian approach and the on-shell parametrizations based on the Watson theorem.

In Sec. II, we define the starting Lagrangian and derive the lowest order Feynman amplitudes for pion photoproduction on the nucleon. In Sec. III, a "three-dimensional reduction" is introduced to express the electromagnetic part of the model Hamiltonian in terms of these Feynman amplitudes. The πN interaction Hamiltonian and the corresponding πN scattering solution will also be presented there. In Sec. IV we demonstrate the unitarity and the gauge invariance of the model. The difference between our formulation and the on-shell parameterization based on the Watson theorem will be explicitly written down in this section. Numerical results and discussions are given in Sec. V. A summary and brief discussion of future developments is presented in Sec. VI.

II. The basic pion photoproduction mechanisms

Following earlier studies,[1-17] we assume that the main features of pion photoproduction can be deduced from an effective Lagrangian describing the interacting fields of the nucleon (ψ_N), delta (ψ^μ_Δ), pion ($\vec{\phi}$), ρ meson ($\vec{\rho}^\mu$), ω meson (ω^μ) and photon (A^μ). We note that here the Δ is a stable bare particle that later obtains it's empirical mass and width by dressing with pions. The interactions involving π, ρ and ω mesons are identical to those considered by Olsson and Osypowski,[5] and therefore take into account chiral symmetry. To describe the electromagnetic coupling of the Δ, we use the formalism of Jones and Scadron.[25] Our interaction Lagrangian can be expressed as

$$\mathcal{L}_{int} = \mathcal{L}_{PV} + \mathcal{L}_{\rho\omega} + \mathcal{L}_{\Delta}. \tag{2.1}$$

The first term, $\mathcal{L}_{PV}$, contains the πN pseudovector coupling contribution, together with related electromagnetic interactions. Using the conventions of Bjorken and Drell,[26] we have

$$\mathcal{L}_{PV} = \mathcal{L}_{\pi NN} + \mathcal{L}_{\gamma NN} + \mathcal{L}_{\gamma\pi\pi} + \mathcal{L}_{\gamma\pi NN}, \tag{2.2a}$$

where

$$\mathcal{L}_{\pi NN} = -\frac{f_{\pi NN}}{m_\pi}\overline{\psi}_N(x)\gamma_5\gamma_\mu\vec{\tau}\psi_N(x)\cdot\partial^\mu\vec{\phi}(x), \tag{2.2b}$$

$$\mathcal{L}_{\gamma NN} = -e_0\overline{\psi}_N(x)\{(\frac{1+\tau_3}{2})\not{A}(x) + [(\frac{1+\tau_3}{2})\frac{\kappa_p}{2m_N} + (\frac{1-\tau_3}{2})\frac{\kappa_n}{2m_N}]\sigma_{\mu\nu}\partial^\mu A^\nu(x)\}\psi_N(x), \tag{2.2c}$$

$$\mathcal{L}_{\gamma\pi\pi} = e_0\{[\partial_\mu\vec{\phi}(x)]^\dagger \times \vec{\phi}(x)\}_3 A^\mu(x), \tag{2.2d}$$

$$\mathcal{L}_{\gamma\pi NN} = -e_0\frac{f_{\pi NN}}{m_\pi}\overline{\psi}_N(x)\gamma_5\gamma_\mu(\vec{\tau}\times\vec{\phi}(x))_3\psi_N(x)A^\mu(x). \tag{2.2e}$$

The second term in Eq. (2.1), $\mathcal{L}_{\rho\omega}$, describes the interactions involving the vector mesons. Explicitly we have

$$\mathcal{L}_{\rho\omega} = \mathcal{L}_{\rho NN} + \mathcal{L}_{\omega NN} + \mathcal{L}_{\rho\pi\gamma} + \mathcal{L}_{\omega\pi\gamma}, \tag{2.3a}$$

where

$$\mathcal{L}_{\rho NN} = f_{\rho NN}\overline{\psi}_N(x)(\gamma_\mu + \frac{K_V}{2m_N}\sigma_{\mu\nu}\partial^\nu)\vec{\tau}\cdot\vec{\rho}^\mu(x)\psi_N(x), \tag{2.3b}$$

$$\mathcal{L}_{\omega NN} = f_{\omega NN}\overline{\psi}_N(x)(\gamma_\mu + \frac{K_S}{2m_N}\sigma_{\mu\nu}\partial^\nu)\vec{\omega}^\mu(x)\psi_N(x), \tag{2.3c}$$

$$\mathcal{L}_{\rho\pi\gamma} = \frac{g_{\rho\pi\gamma}}{m_\pi}\epsilon_{\alpha\beta\gamma\delta}\partial^\alpha A^\beta(x)\vec{\phi}(x)\cdot\partial^\gamma\vec{\rho}^\delta(x), \tag{2.3d}$$

$$\mathcal{L}_{\omega\pi\gamma} = \frac{g_{\omega\pi\gamma}}{m_\pi}\epsilon_{\alpha\beta\gamma\delta}\partial^\alpha A^\beta(x)\phi_3(x)\partial^\gamma\omega^\delta(x). \tag{2.3e}$$

The last term of Eq. (2.1), $\mathcal{L}_\Delta$, involves the Δ-excitation. It is given by

$$\mathcal{L}_\Delta = \mathcal{L}_{\pi N\Delta} + \mathcal{L}_{\gamma N\Delta}, \tag{2.4a}$$

where

$$\mathcal{L}_{\pi N\Delta} = \frac{f_{\pi N\Delta}}{m_\pi}\overline{\psi}^\mu_\Delta(x)\vec{T}\psi_N(x)\cdot\partial_\mu\vec{\phi}(x) + h.c., \tag{2.4b}$$

$$\mathcal{L}_{\gamma N\Delta} = ie_0\overline{\psi}^\mu_\Delta(x)T_3\Gamma_{\mu\nu}\psi_N(x)A^\nu(x) + h.c. \tag{2.4c}$$

with

$$T_i^\dagger T_j = \frac{2}{3}\delta_{ij} - \frac{i}{3}\epsilon_{ijk}\tau_k. \qquad (i,j,k = 1,2,3). \tag{2.4d}$$

In Eq. (2.4c) $\Gamma_{\mu\nu}$ is a $\gamma N \leftrightarrow \Delta$ vertex which we discuss later in this section.

In Eqs. (2.2)–(2.4), the isospin operator $\vec{\tau}$ is the usual 2×2 Pauli operator, while $\vec{T}$ is the $N \to \Delta$ isospin transition operator. The charged fields of the pion are defined as

$$\phi_\pm = \mp\frac{1}{\sqrt{2}}(\phi_1 \pm i\phi_2), \tag{2.5a}$$

$$\phi_0 = \phi_3. \tag{2.5b}$$

Note that this convention differs from that of Bjorken and Drell by a $(-)$ sign for the ϕ_+ state. Accordingly we define

$$\tau_\pm = \mp\frac{1}{\sqrt{2}}(\tau_1 \pm i\tau_2), \tag{2.6a}$$

$$\tau_0 = \tau_3 \tag{2.6b}$$

and hence

$$\vec{\tau}\cdot\vec{\phi} = \tau_0\phi_0 - \tau_-\phi_+ - \tau_+\phi_-. \tag{2.7}$$

This choice, more conventionally used in nuclear physics, makes the pion field a usual spherical vector and allows us to calculate isospin matrix elements using standard tensor algebra, as given, for example, in the book by Brink and Satchler.[27] Similar relations are used to define the charge states of the ρ meson.

Starting from the Lagrangians of Eqs. (2.1)–(2.4), it is straightforward to calculate the lowest order Feynman amplitudes for photoproduction of a πN state from a nucleon. The kinematics of these Feynman amplitudes are given in Fig. 1. Amplitudes of Figs. 1(a)-1(f) are traditionally called the "Born terms". Using the Lagrangian $\mathcal{L}_{PV}+\mathcal{L}_{\rho\omega}$ we write the Born amplitudes of the $\gamma+N(\tau) \rightarrow \pi^\alpha+N(\tau')$ reaction as

$$M_\alpha^{Born} = < \pi^\alpha(k), N(p',s',\tau') \mid J_\mu^{Born}(0) \mid N(p,s,\tau) > \epsilon^\mu(q,\lambda), \qquad (2.8a)$$

where $\epsilon^\mu(q,\lambda)$ is the photon polarization vector with helicity λ, and α is the isospin projection of the pion. The spin and isospin projections of the initial (final) nucleon are denoted by s (s') and τ (τ'), respectively. For the charged pions we obtain

$$\begin{aligned}
&< \pi^\pm(k), N(p',s',\tau') \mid J_\mu^{Born}(0) \mid N(p,s,\tau) > \\
&= i\overline{u}_N(p',s',\tau')[\\
&\pm e_0 \frac{f_{\pi NN}}{m_\pi} \tau_{\mp 1} \{ -\gamma_5\gamma_\mu + \gamma_5(\not{k}-\not{q})(2k-q)_\mu \Delta_F(k-q) \} \\
&+ e_0 \frac{f_{\pi NN}}{m_\pi} \tau_{\mp 1}\gamma_5 \not{k} S_F(p+q) \{ (\frac{1+\tau_3}{2})\gamma_\mu + [(\frac{1+\tau_3}{2})\frac{\kappa_p}{2m_N} + (\frac{1-\tau_3}{2})\frac{\kappa_n}{2m_N}] i\sigma_{\mu\nu}q^\nu \} \\
&+ e_0 \frac{f_{\pi NN}}{m_\pi} \{ (\frac{1+\tau_3}{2})\gamma_\mu + [(\frac{1+\tau_3}{2})\frac{\kappa_p}{2m_N} + (\frac{1-\tau_3}{2})\frac{\kappa_n}{2m_N}] i\sigma_{\mu\nu}q^\nu \} S_F(p'-q) \gamma_5 \not{k} \tau_{\mp 1} \\
&\quad - g_{\rho\pi\gamma} \frac{f_{\rho NN}}{m_\pi} \tau_{\mp 1} \{ \gamma_\lambda + \frac{K_V}{2m_N} i\sigma_{\lambda\nu}(k-q)^\nu \} i\epsilon_{\mu\alpha\beta\gamma} k^\alpha q^\beta D_F^{\gamma\lambda}(k-q;\rho) \\
&\quad\quad] u_N(p,s,\tau), \qquad (2.8b)
\end{aligned}$$

and for the neutral pion we have

$$\begin{aligned}
&< \pi^0(k), N(p',s',\tau') \mid J_\mu^{Born}(0) \mid N(p,s,\tau) > \\
&= i\overline{u}_N(p',s',\tau')[\\
&- e_0 \frac{f_{\pi NN}}{m_\pi} \tau_3\gamma_5 \not{k} S_F(p+q) \{ (\frac{1+\tau_3}{2})\gamma_\mu + [(\frac{1+\tau_3}{2})\frac{\kappa_p}{2m_N} + (\frac{1-\tau_3}{2})\frac{\kappa_n}{2m_N}] i\sigma_{\mu\nu}q^\nu \} \\
&- e_0 \frac{f_{\pi NN}}{m_\pi} \{ (\frac{1+\tau_3}{2})\gamma_\mu + [(\frac{1+\tau_3}{2})\frac{\kappa_p}{2m_N} + (\frac{1-\tau_3}{2})\frac{\kappa_n}{2m_N}] i\sigma_{\mu\nu}q^\nu \} S_F(p'-q) \gamma_5 \not{k} \tau_3 \\
&+ g_{\rho\pi\gamma} \frac{f_{\rho NN}}{m_\pi} \tau_3 \{ \gamma_\lambda + \frac{K_V}{2m_N} i\sigma_{\lambda\nu}(k-q)^\nu \} i\epsilon_{\mu\alpha\beta\gamma} q^\alpha k^\beta D_F^{\gamma\lambda}(k-q;\rho) \\
&\quad + g_{\omega\pi\gamma} \frac{f_{\omega NN}}{m_\pi} \{ \gamma_\lambda + \frac{K_S}{2m_N} i\sigma_{\lambda\nu}(k-q)^\nu \} i\epsilon_{\mu\alpha\beta\gamma} q^\alpha k^\beta D_F^{\gamma\lambda}(k-q;\omega) \\
&\quad\quad] u_N(p,s,\tau). \qquad (2.8c)
\end{aligned}$$

In the above equations, all notation for nucleon spinors, propagators, etc., is identical to that of Bjorken and Drell.[26]

Next we write the $\gamma+N(\tau) \rightarrow \Delta(\tau_\Delta)$ amplitude using the Lagrangian $\mathcal{L}_{\gamma N\Delta}$ of Eq. (2.4c) as

$$M^\Delta = < \Delta(p_\Delta,s_\Delta,\tau_\Delta) \mid J_\mu^\Delta(0) \mid N(p,s,\tau) > \epsilon^\mu(q,\lambda) \qquad (2.9a)$$

where

$$\begin{aligned}
&< \Delta(p_\Delta,s_\Delta,\tau_\Delta) \mid J_\mu^\Delta(0) \mid N(p,s,\tau) > \\
&= ie_0 (1/2,\tau,1,0 \mid 3/2,\tau_\Delta) \overline{w}^\nu(p_\Delta,s_\Delta) \Gamma_{\nu\mu} u_N(p,s). \qquad (2.9b)
\end{aligned}$$

The Rarita-Schwinger spinor $w^\mu(p_\Delta,s_\Delta)$ in Eq. (2.9b) is defined by

$$w^\mu(p_\Delta,s_\Delta) = \sum_{m'',s''} (1,m'',1/2,s'' \mid 3/2,s_\Delta) \epsilon_{m''}^\mu(\vec{p}_\Delta) u_\Delta(p_\Delta,s'') \qquad (2.9c)$$

where $u_\Delta(p_\Delta,s'')$ is a spin 1/2 spinor with a spin projection s'' and a bare Δ-mass $m_{0\Delta}$. The spin 1 four-vector $\epsilon_m^\mu(\vec{p}_\Delta)$ is given by

$$\begin{aligned}
&\epsilon_m^\mu(\vec{p}_\Delta) = (\epsilon_m^0(\vec{p}_\Delta), \vec{\epsilon}_m(\vec{p}_\Delta)), \\
&\epsilon_m^0(\vec{p}_\Delta) = \frac{p_{\Delta m}}{m_{0\Delta}}, \qquad \vec{\epsilon}_m(\vec{p}_\Delta) = \hat{\epsilon}_m + \frac{p_{\Delta m}}{m_{0\Delta}} \frac{\vec{p}_\Delta}{E_\Delta(p_\Delta)+m_{0\Delta}}, \qquad m = \pm 1, 0, \qquad (2.9d) \\
&\hat{\epsilon}_{\pm 1} = \mp \frac{1}{\sqrt{2}} (1, \pm i, 0) \qquad and \qquad \hat{\epsilon}_0 = (0,0,1).
\end{aligned}$$

We follow Jones and Scadron[25] to define the $\gamma N \leftrightarrow \Delta$ vertex as

$$\Gamma_{\mu\nu} = G_M(q^2) K_{\mu\nu}^M + G_E(q^2) K_{\mu\nu}^E, \qquad (2.10a)$$

with

$$\begin{aligned}
K_{\mu\nu}^M &= -\frac{3}{\{(m_{0\Delta}+m_N)^2 - q^2\}} \epsilon_{\mu\nu\alpha\beta} P^\alpha q^\beta \frac{(m_{0\Delta}+m_N)}{2m_N}, \qquad (2.10b) \\
K_{\mu\nu}^E &= -K_{\mu\nu}^M - \frac{6}{\{(m_{0\Delta}+m_N)^2 - q^2\}\{(m_{0\Delta}-m_N)^2 - q^2\}} \\
&\qquad \epsilon_{\mu\lambda\alpha\beta} P^\alpha q^\beta \epsilon_\nu{}^\lambda{}_{\gamma\delta} p_\Delta^\gamma q^\delta i\gamma_5 \frac{(m_{0\Delta}+m_N)}{m_N}, \qquad (2.10c)
\end{aligned}$$

where q ($= p_\Delta - p$) is the photon momentum and $P = (p+p_\Delta)/2$. In Eq. (2.10a) we dropped a term proportional to the charged form factor $G_C(q^2)$, since it does not contribute to the photoproduction reaction. Note that the form factors $G_M(q^2)$ and $G_E(q^2)$ in Eq. (2.10a) are bare form factors which get dressed by

pions on inclusion of final state interactions. The Δ-excitation vertex is used in calculating the diagram of Fig. 1(g).

Eqs. (2.8)-(2.10) define the basic pion photoproduction mechanisms on the nucleon. Apart from the Δ excitation parameters $G_M(0)$ and $G_E(0)$, all parameters are taken from the literature and are listed in Table 1. In the next section we will show how the current matrix elements defined in this section are used in defining the model Hamiltonian in terms of only the pion, the nucleon and the Δ degrees of freedom.

III. $\gamma N \to \pi N$ scattering equations

Although we restrict our attention to photoproduction off one nucleon, this can be considered a first step at extending the unitary models of few-body hadronic systems[18-22] to the electromagnetic sector. With this in mind, it is desirable to derive scattering equations for photoproduction with the same methods as used for the few-body models. Motivated by the πNN formulation of Refs. 18-20, one such derivation has been given by Afnan and Araki[17] using diagramatic techniques. The resulting equations have sometimes been used in the past,[10,11,14] but usually without explicit proof. Here we present an alternative derivation starting from a model Hamiltonian. The present work is closer in sprit to the Hamiltonian formulation of the πNN system developed in Refs. 21-22.

We retain four explicit channels, πN, γN, N, and Δ. States with a higher number of pions are implicitly taken into account through potentials. Thus our Hilbert space can be written in terms of direct sums of channel subspaces

$$\mathcal{H} = S \oplus \gamma N, \tag{3.1a}$$

$$S = \sum_{B=N,\Delta} \pi N \oplus B. \tag{3.1b}$$

Subspace S describes pion nucleon scattering without coupling to photons, and needs to be discussed first. The assumed model Hamiltonian in this subspace takes the form

$$H_S = H_0 + H_I \tag{3.2a}$$

with

$$H_0 = \int d\vec{k}\, E_\pi(\vec{k})\, a^\dagger_{\vec{k}} a_{\vec{k}} + \sum_{B=N,\Delta} \int d\vec{p}\, E_B(\vec{p})\, b^\dagger_{\vec{p}B} b_{\vec{p}B}. \tag{3.2b}$$

Here $a^\dagger_{\vec{k}}$ and $b^\dagger_{\vec{p}B}$ are respectively the creation operator of a pion with a momentum $\vec{k}$, and a baryon $B(= N$ or $\Delta)$ with a momentum $\vec{p}$. All spin-isospin indices are suppressed here. We define $E_\pi(\vec{k}) = \sqrt{\vec{k}^2 + m_\pi^2}$, $E_B(p) = \sqrt{\vec{p}^2 + m_{0B}^2}$ with m_{0B} being the bare mass of the baryon B. Strictly speaking, however, Eq. (3.2b) only applies to a theory with multi-pion states. Since our Hilbert space contains at most one pion states, the nucleon in a πN state will not be explicitly dressed. For this reason, we use the physical nucleon mass in Eq. (3.2b) for all states in subspace πN.

The interaction term is written as

$$H_I = \sum_{B=N,\Delta} [\int d\vec{p}\,' d\vec{p} d\vec{k}\, a^\dagger_{\vec{k}} b^\dagger_{\vec{p}\,'N} b_{\vec{p}B}\, f^0_{\pi N,B}(\vec{k},\vec{p}\,',\vec{p})$$

$$+ \int d\vec{p}\,' d\vec{p} d\vec{k}' d\vec{k}\; b^{\dagger}_{\vec{p}\,'N} b_{\vec{p}N} a^{\dagger}_{\vec{k}'} a_{\vec{k}}\; v_{\pi N,\pi N}(\vec{p}\,'\vec{k}', \vec{p}, \vec{k}) \;] \quad + h.c. \qquad (3.2c)$$

The form of the Hamiltonian in Eqs. (3.2) is identical to that deduced from the cloudy bag model.[23] Thus in principle, one can use the cloudy bag model values for both the vertices $f^0_{\pi N,B}$ and the pion-nucleon potential $v_{\pi N,\pi N}$. Using this Hamiltonian, the Lippmann-Schwinger equation in the subspace S is

$$T = H_I + H_I G_0 T, \qquad (3.3a)$$

where

$$G_0 = \frac{1}{E - H_0 + i\epsilon}. \qquad (3.3b)$$

Using the completeness relation

$$\sum_{B=N,\Delta} |B >< B| + |\pi N >< \pi N| = 1, \qquad (3.4)$$

and taking matrix elements of Eq. (3.3a) between states $|\pi N >$ and $|B >$, we get the coupled equations

$$T_{\pi N,\pi N} = v_{\pi N,\pi N} + v_{\pi N,\pi N} G_{\pi N} T_{\pi N,\pi N} + \sum_{B=N,\Delta} f^0_{\pi N,B} g^0_B T_{B,\pi N} \qquad (3.5a)$$

$$T_{B,\pi N} = f^0_{B,\pi N} + f^0_{B,\pi N} G_{\pi N} T_{\pi N,\pi N}. \qquad (3.5b)$$

On substitution, these give the following one-channel Lippmann-Schwinger equation

$$T_{\pi N,\pi N} = V_{\pi N,\pi N} + V_{\pi N,\pi N} G_{\pi N} T_{\pi N,\pi N} \qquad (3.6a)$$

where

$$V_{\pi N,\pi N} = \sum_{B=N,\Delta} f^0_{\pi N,B} g^0_B f^0_{B,\pi N} + v_{\pi N,\pi N}. \qquad (3.6b)$$

In the above, we have written $G_{\pi N}$ for the free propagator in subspace πN, and g^0_B for the free propagator in subspace B. In the centre of mass (c.m.) system, they take the form

$$< \vec{k}'|G_{\pi N}(E)|\vec{k} > = \frac{1}{E - E_N(\vec{k}) - E_\pi(\vec{k}) + i\epsilon}\delta(\vec{k} - \vec{k}'), \qquad (3.7a)$$

$$g^0_B(E) = \frac{1}{E - m_{0B}}. \qquad (3.7b)$$

With some further algebra,[29] one can reexpress the πN t-matrix as

$$T_{\pi N,\pi N}(E) = T^{NP}_{\pi N,\pi N}(E) + \sum_{B=N,\Delta} f_{\pi N,B}(E) g_B(E) f_{B,\pi N}(E), \qquad (3.8)$$

where the non-pole (NP) amplitude $T^{NP}_{\pi N,\pi N}$ is determined by the Lippmann-Schwinger equation

$$T^{NP}_{\pi N,\pi N}(E) = v_{\pi N,\pi N} + v_{\pi N,\pi N} G_{\pi N}(E) T^{NP}_{\pi N,\pi N}(E). \qquad (3.9)$$

The second term on the right hand side of Eq. (3.8) describes the formation of a dressed baryon and its propagation. The dressed vertex function $f_{\pi N,B}(E)$ takes the form

$$f_{\pi N,B}(E) = f^0_{\pi N,B} + T^{NP}_{\pi N,\pi N}(E) G_{\pi N}(E) f^0_{\pi N,B}. \qquad (3.10)$$

The dressed baryon propagator $g_B(E)$ in Eq. (3.8) is determined by the bare mass m_{0B} of the baryon and a self-energy term

$$g_B(E) = \frac{1}{E - m_{0B} - \Sigma_B(E)} \qquad (3.11)$$

with

$$\Sigma_B(E) = f^0_{B,\pi N} G_{\pi N}(E) f^0_{\pi N,B} + f^0_{B,\pi N} G_{\pi N}(E) T^{NP}_{\pi N,\pi N}(E) G_{\pi N}(E) f^0_{\pi N,B}. \qquad (3.12)$$

For the P_{11} and P_{33} channels, the model obviously should yield

$$m_N = m_{0N} + \Sigma_N(m_N) \qquad (3.13a)$$

and

$$m_\Delta \equiv E_R + \frac{i}{2}\Gamma_R = m_{0\Delta} + \Sigma_\Delta(m_\Delta). \qquad (3.13b)$$

Here m_N is the physical nucleon mass, E_R=1236 MeV and Γ_R=115 MeV.

For the P_{33} channel, we follow the cloudy bag model study of Ref. 23 to parametrize the vertex as

$$f^0_{\pi N\Delta}(k) = \frac{f_{\pi N\Delta}}{m_\pi} \frac{k}{(2\pi)^{3/2}\sqrt{2E_\pi(k)}} e^{-c(kR)^2} \qquad (3.14)$$

where c=0.106 fm^{-2} and R is the bag radius. One of our objectives in this work is to examine the dependence of the $\gamma N \to \pi N$ cross section on the bag radius R. The potential $v_{\pi N,\pi N}$ represents πN interactions due to intermediate states with more than one pion, as well as possible short range interactions. An accurate description of this term is beyond the cloudy bag model, and we are lead to simply parametrize $v_{\pi N,\pi N}$ as a separable potential. We retain all s-, p- and d-wave πN channels. A more detailed discussion of our description of πN scattering is presented in Appendix A.

Before we introduce the electromagnetic interaction, it is important to note that in the above πN formulation all particles are restricted on their mass-shell,

although during the collisions the system can be off its energy-shell. It is certainly not a covariant field theoretical formulation. As is well known, this is at present an unavoidable approximation for "deducing" from a field theory a practical model which can confront experimental data. Our next task is to find a way to implement the electromagnetic interactions, defined in Sec. II, into this "three-dimensional" formulation. For this we'll use gauge invariance as the guiding principle.

The electromagnetic interaction can be introduced by adding a terms to the πN Hamiltonian H_S

$$H = H_S + H_0^{em} + H_I^{em} \tag{3.15a}$$

where H_0^{em} is the free photon Hamiltonian, and

$$H_I^{em} = \int d\vec{x} A^\mu(x) j_\mu(x), \tag{3.15b}$$

is expressed in terms of the electromagnetic current operator $j_\mu(x)$. By translational invariance, the coordinate-dependence of the current operator is trivial

$$j_\mu(x) = e^{-iP\cdot x} j_\mu(0) e^{iP\cdot x}, \tag{3.16}$$

where P is the total four momentum operator of the system. We now assume that the matrix elements of $j_\mu(0)$ in the subspace $B \bigoplus \pi N$ are the Feynman amplitudes defined by Eqs. (2.8)-(2.9), evaluated at the on-mass-shell limit, and multiplied by phase space factors Eqs. (C.5). Namely, all four momenta of the external legs in Fig. 1 are set to be $p^2 = p'^2 = m_N^2$ for the nucleon and $k^2 = m_\pi^2$ for the pion. Note that this "three-dimensional reduction" leads to an ambiguity in defining the four momentum of the intermediate state if the transition is off the energy-shell. For example the matrix elements of Fig. 1(a) evaluated with $p_0'' = q_0 + E_N(\vec{p})$ and $p_0'' = E_\pi(\vec{k}) + E_N(\vec{p}')$ are different for the off-energy-shell kinematics. This is precisely the reason why the gauge invariance of the original Lagrangian formulation becomes hidden and may be destroyed in the three-dimensional theory if the choice of the intermediate four momentum is not properly made. We will explain this in more detail in the next section where the gauge invariance of our formulation will be proved.

With the above assumptions, the Hamiltonian H_I^{em} can be written as

$$\begin{aligned} H_I^{em} = & \int d\vec{k} d\vec{p}' d\vec{q} d\vec{p}\, a_{\vec{k}}^\dagger b_{\vec{p}'N}^\dagger v_{\pi N,\gamma N}^{Born}(\vec{k}\vec{p}', \vec{q}\vec{p}) c_{\vec{q}\lambda} b_{\vec{p}N} \\ & + \int d\vec{p}' d\vec{q} d\vec{p}\, b_{\vec{p}'\Delta}^\dagger f_{\Delta,\gamma N}^0(\vec{p}', \vec{q}\vec{p}) c_{\vec{q}\lambda} b_{\vec{p}N} \\ & + \int d\vec{q}' d\vec{p}' d\vec{q} d\vec{p}\, c_{\vec{q}'\lambda'}^\dagger b_{\vec{p}'N}^\dagger v_{\gamma N,\gamma N}^{Born}(\vec{q}'\vec{p}', \vec{q}\vec{p}) c_{\vec{q}\lambda} b_{\vec{p}N} \end{aligned} \tag{3.17}$$

where $c_{\vec{q}\lambda}$ ($c_{\vec{q}\lambda}^\dagger$) is the annihilation (creation) operator for photons of momentum $\vec{q}$ and helicity λ, and

$$v_{\pi N,\gamma N}^{Born}(\vec{k}\vec{p}', \vec{q}\vec{p}) = (2\pi)^3 F_{cut}(\vec{k}_{\pi N}) F_\pi(\vec{k}) F_N(\vec{p}') F_\gamma(\vec{q}) F_N(\vec{p})\, M^{Born}, \tag{3.18a}$$

$$f_{\Delta,\gamma N}^0(\vec{p}', \vec{q}\vec{p}) = (2\pi)^{3/2} F_\Delta(\vec{p}') F_\gamma(\vec{q}) F_N(\vec{p})\, M^\Delta. \tag{3.18b}$$

Here M^{Born} and M^Δ are current matrix elements which have been given explicitly in Eqs. (2.8)-(2.9), and as discussed in Appendix C, $F_\pi(\vec{k})$, $F_N(\vec{p})$, and $F_\gamma(\vec{q})$ are phase-space factors (explicitly given in Eqs. (C.5)) required by changing the covariant normalization of Bjorken and Drell[26] to the non-covariant normalization of Goldberger and Watson.[30] Eq. (3.18b) arises explicitly by comparing non-relativistic expressions for $f_{\pi N,\Delta}^0 g_\Delta^0 f_{\Delta,\pi N}^0$ and $f_{\pi N,\Delta}^0 g_\Delta^0 f_{\Delta,\gamma N}^0$ with those using the Rarita-Schwinger formalism. Here the Δ phase-space factor is only slightly modified

$$F_\Delta(\vec{p}_\Delta) = \frac{1}{(2\pi)^{3/2}} \left(\frac{E_\Delta(\vec{p}_\Delta) + m_\Delta}{2m_\Delta}\right) \sqrt{\frac{m_\Delta}{E_\Delta(\vec{p}_\Delta)}}. \tag{3.19a}$$

In Eq. (3.17), the term $v_{\gamma N,\gamma N}^{Born}(\vec{q}'\vec{p}', \vec{q}\vec{p})$ contributes to Compton scattering. Since it's effect on pion photoproduction is negligible, we shall not discuss it in detail here. Note that in Eqs. (3.18) a cutoff function F_{cut} is introduced to make the Born term a square integrable operator. It is defined by

$$F_{cut}(\vec{k}_{\pi N}) = \left(\frac{\Lambda^2}{\Lambda^2 + \vec{k}_{\pi N}^2}\right) \tag{3.19b}$$

where $\vec{k}_{\pi N}$ is the πN relative momentum, and Λ is a cutoff parameter which will be determined by fitting pion photoproduction data. Here we assumed that all Born terms have the same cutoff form factor. This is of course not very satisfactory. It is desirable to associate a different form factor with each vertex shown in Fig. 1, according to the cloudy bag model. In practice, however, it is difficult to achieve, since the model will lead to a violation of gauge invariance. Both gauge invariance and unitarity of our model will be verified in the next section.

In comparing the interaction Hamiltonians of Eqs. (3.2c) and (3.17), it is apparent that transitions to subspace N are handled differently in the two cases. The strong interaction Hamiltonian of Eq. (3.2c) is expressed in terms of a "background" potential $v_{\pi N,\pi N}$ that does not have a pole at the (bare) nucleon mass. Instead, an explicit vertex $f_{\pi N,N}^0$ is included. Ideally, the electromagnetic Hamiltonian of Eq.(3.17) should be handled similarly. That is, the nucleon pole diagram of Fig. 1(a) should be excluded from the term $v_{\gamma N,\pi N}^{Born}$, and an explicit vertex $f_{\gamma N,N}^0$ should appear in Eq. (3.17). It is clear, however, that maintaining gauge

invariance would be difficult under such a scheme. Because of the importance of gauge invariance, we have rather chosen to keep the Born term intact, and exclude an explicit $f^0_{\gamma N,N}$ vertex from H_I^{em}. This inconsistency leads to nucleon "overdressing" when final state interactions in the P_{11} channel are included in the diagram of Fig.1(a). For the P_{11} interaction that we use (specified in Table 2), this overdressing leads to a very small mass shift in the nucleon propagator and is therefore expected to be insignificant to our numerical calculations of photoproduction observables.

The scattering equations for $\gamma N \to \pi N$ can now be derived using the same procedure as for πN scattering. Using the Hamiltonian of Eq. (3.15), we write the Lippmann-Schwinger equation in the full Hilbert space $\mathcal{H}$ as

$$T = H + TGH. \tag{3.20}$$

Here the completeness relation is

$$\sum_{B=N,\Delta} |B><B| + |\pi N><\pi N| + |\gamma N><\gamma N| = 1. \tag{3.21}$$

Taking matrix elements of Eq. (3.20) between states $|\gamma N>$ and $|\pi N>$, using Eq. (3.5b), and keeping only the lowest order electromagnetic contribution, leads to the following equations for pion photoproduction:

$$T_{\pi N,\gamma N} = V_{\pi N,\gamma N} + T_{\pi N,\pi N} G_{\pi N} V_{\pi N,\gamma N}, \tag{3.22a}$$

$$V_{\pi N,\gamma N} = v^{Born}_{\pi N,\gamma N} + v^{\Delta}_{\pi N,\gamma N}, \tag{3.22b}$$

$$v^{\Delta}_{\pi N,\gamma N} = f^0_{\pi N,\Delta} g^0_{\Delta} f^0_{\Delta,\gamma N}. \tag{3.22c}$$

Here $v^{Born}_{\pi N,\gamma N}$ and $f^0_{\Delta,\gamma N}$ are defined in Eqs. (3.18), and g^0_{Δ} is defined in Eq. (3.7b). Eqs. (3.22) can also be cast into familiar resonance (Δ) plus non-resonance (NR) parts

$$T_{\pi N,\gamma N} = T^{NR}_{\pi N,\gamma N} + \frac{f_{\pi N,\Delta} f^0_{\Delta,\gamma N}}{E - m_{0\Delta} - \Sigma_{\Delta}(E)}, \tag{3.23a}$$

with

$$T^{NR}_{\pi N,\gamma N} = v^{Born}_{\pi N,\gamma N} + T_{\pi N,\pi N} G_{\pi N} v^{Born}_{\pi N,\gamma N}, \tag{3.23b}$$

where the dressed vertex $f_{\pi N,\Delta}$ is defined in Eq. (3.10) and the self-energy $\Sigma_{\Delta}(E)$ is defined in Eq. (3.12). This completes our derivation of the pion photoproduction amplitude. We finally note that the above procedure also leads to equations for Compton scattering. Indeed, retaining all orders in e, one obtains a coupled set of equations for the processes $\pi N \to \pi N$ $\pi N \to \gamma N$ and $\gamma N \to \gamma N$ which can be written in matrix form as

$$\begin{pmatrix} T_{\pi N,\pi N} & T_{\pi N,\gamma N} \\ T_{\gamma N,\pi N} & T_{\gamma N,\gamma N} \end{pmatrix} = \begin{pmatrix} V_{\pi N,\pi N} & V_{\pi N,\gamma N} \\ V_{\gamma N,\pi N} & V_{\gamma N,\gamma N} \end{pmatrix}$$
$$+ \begin{pmatrix} V_{\pi N,\pi N} & V_{\pi N,\gamma N} \\ V_{\gamma N,\pi N} & V_{\gamma N,\gamma N} \end{pmatrix} \begin{pmatrix} G_{\pi N} & 0 \\ 0 & G_{\gamma N} \end{pmatrix} \begin{pmatrix} T_{\pi N,\pi N} & T_{\pi N,\gamma N} \\ T_{\gamma N,\pi N} & T_{\gamma N,\gamma N} \end{pmatrix} \tag{3.24}$$

where

$$V_{\pi N,\pi N} = \sum_{B=N,\Delta} f^0_{\pi N,B} g^0_B f^0_{B,\pi N} + v_{\pi N,\pi N}\ , \tag{3.25a}$$

$$V_{\pi N,\gamma N} = f^0_{\pi N,\Delta}\ g^0_{\Delta}\ f^0_{\Delta,\gamma N}\ + v^{Born}_{\pi N,\gamma N}\ , \tag{3.25b}$$

$$V_{\gamma N,\pi N} = f^0_{\gamma N,\Delta}\ g^0_{\Delta}\ f^0_{\Delta,\pi N}\ + v^{Born}_{\gamma N,\pi N}\ , \tag{3.25c}$$

$$V_{\gamma N,\gamma N} = f^0_{\gamma N,\Delta}\ g^0_{\Delta}\ f^0_{\Delta,\gamma N}\ + v^{Born}_{\gamma N,\gamma N}\ . \tag{3.25d}$$

In the next section, Eqs. (3.24) and (3.25) will serve as the basis for proving the unitarity of our formulation.

IV. Pion photoproduction amplitude: unitarity and gauge invariance

In the first part of this section we will show that the $\gamma N \to \pi N$ model, described in Sec. III, satisfies unitarity (up to the first order of electromagnetic coupling constant e_0), and hence the Watson theorem.[24] More importantly, we will show that its dynamical content is significantly different from that of the early approaches[5-9] using solely the Watson theorem to describe the πN final state interaction. In the second part we explicitly prove, that for a particular choice of intermediate state momentum variables, the present Hamiltonian formulation is gauge invariant.

For the case of pion photoproduction, consequences of unitarity are well discussed in standard texts.[30] However, it will be useful to present some of the arguments here. Unitarity of the S-matrix, i.e.

$$SS^\dagger = 1, \tag{4.1}$$

is assumed to hold in the Hilbert space $\pi N \oplus \gamma N$. Taking matrix elements of Eq. (4.1) between states $< \pi N|$ and $|\gamma N >$, and keeping only the lowest orders in e_0, leads to the relation

$$S_{\pi N,\gamma N} + S_{\pi N,\pi N} S^*_{\gamma N,\pi N} = 0. \tag{4.2}$$

In terms of the partial wave t-matrix, defined as in Appendix C, Eq. (4.2) becomes

$$T^{\ell jt,L}_{\pi N,\gamma N}(k,q,E) - T^{\ell jt,L}_{\pi N,\gamma N}{}^*(k,q,E) = -2\pi i \rho(k_0) T^{\ell jt}_{\pi N,\pi N}(k,k_0,E) T^{\ell jt,L}_{\pi N,\gamma N}{}^*(k_0,q,E). \tag{4.3}$$

where, at this stage, $k_0 = k$, and *all momenta are on-energy-shell.* In the derivation of Eq. (4.3) we have used time reversal invariance of the t-matrix. Here ℓjt specifies the πN partial wave, L is the corresponding allowed photon orbital angular momentum, and ρ is defined in Eq. (C.7). By noting Eq. (C.6), we see that Eq. (4.3) is equivalent to

$$T^{\ell jt,L}_{\pi N,\gamma N}(k,q,E) = e^{i\delta^{jt}_\ell} |T^{\ell jt,L}_{\pi N,\gamma N}(k,q,E)| \tag{4.4}$$

which is the statement of Watson's theorem.

The equations for pion photoproduction are given by Eqs. (3.22). One way to prove unitarity, however, is to start with the matrix equation (3.24) for the fully coupled processes of $\pi N \to \pi N$, $\gamma N \to \pi N$, and $\gamma N \to \gamma N$. These equations define a Lippmann-Schwinger equation in the space $\pi N \oplus \gamma N$:

$$\tilde{T}(E) = \tilde{V}(E) + \tilde{V}(E)\tilde{G}(E)\tilde{T}(E) \tag{4.5}$$

where the tildes serve to indicate that these are 2×2 matrices. We now can follow the usual procedure to show the unitarity of a Lippmann-Schwinger equation. Formal manipulation of Eq. (4.5) gives a relation for the unitarity cut

$$\tilde{T}(E^+) - \tilde{T}(E^-) = \tilde{T}(E^+)[\tilde{V}(E^+)^{-1} - \tilde{V}(E^-)^{-1}]\tilde{T}(E^-)$$

$$+\tilde{T}(E^+)[\tilde{G}(E^+) - \tilde{G}(E^-)]\tilde{T}(E^-). \tag{4.6}$$

For pion photoproduction we need only the (1,2) element of Eq. (4.6). Dropping the higher order electromagnetic term, we obtain

$$T_{\pi N,\gamma N}(E^+) - T_{\pi N,\gamma N}(E^-) = T_{\pi N,\pi N}(E^+)[G_{\pi N}(E^+) - G_{\pi N}(E^-)]T_{\pi N,\gamma N}(E^-). \tag{4.7}$$

After performing a partial wave decomposition, and noting that all potentials of Eq. (3.25) are real functions of energy, we again obtain Eq. (4.3). This time, however, the momenta k and q can be off-energy-shell, while k_0 remains at its on-shell value. In this case Eq. (4.3) can be referred to as the *off-shell unitarity relation*; for k and q on-shell, this reduces to the usual statement of unitarity.

The dynamic content of our model can be shown more clearly by introducing the well known relations

$$T_{\pi N,\pi N}(E) = R_{\pi N,\pi N}(E) - i\pi T_{\pi N,\pi N}(E)\delta(E-H_0)R_{\pi N,\pi N}(E), \tag{4.8a}$$

$$\frac{1}{E - H_0 \pm i\epsilon} = \mp i\pi\delta(E - H_0) + \frac{\wp}{E - H_0}, \tag{4.8b}$$

where $\wp$ means taking the principal-value in evaluating the propagator. $R_{\pi N,\pi N}(E)$ is the reaction matrix which is an hermitian operator defined by

$$R_{\pi N,\pi N}(E) = H_I + H_I \frac{\wp}{E - H_0 - H_I} H_I, \tag{4.8c}$$

where H_I is defined by Eq. (3.2c). After partial-wave decomposition, the half-off-shell πN matrix element of Eq. (4.8a) is

$$T^{\ell jt}_{\pi N,\pi N}(k_0,k,E) = R^{\ell jt}_{\pi N,\pi N}(k_0,k,E) - i\pi\rho(k_0) T^{\ell jt}_{\pi N,\pi N}(k_0,k_0,E) R^{\ell jt}_{\pi N,\pi N}(k_0,k,E), \tag{4.9}$$

Note that the half-off-shell t-matrix has been expressed in terms of the on-shell t-matrix and half-off-shell R-matrix which is a real function because of its hermiticity. By using Eq. (4.8b) to evaluate the πN propagator in Eq. (3.22), and using the relations Eqs. (C.6) and (4.9) to perform the partial-wave decomposition, the pion photoproduction amplitude of a given partial wave can be written as

$$T^{\ell jt,L}_{\pi N,\gamma N}(k_0,q,E) = e^{i\delta^{jt}_\ell} \cos\delta^{jt}_\ell \, [\, V^{\ell jt,L}_{\pi N,\gamma N}(k_0,q,E) \; + \; (PV)\,] \tag{4.10}$$

where

$$(PV) = \wp \int dk k^2 \frac{R^{\ell jt}_{\pi N,\pi N}(k_0,k,E)}{E - E_N(k) - E_\pi(k)} V^{\ell jt,L}_{\pi N,\gamma N}(k,q,E). \tag{4.11}$$

A key point to note is that the partial wave matrix elements $R^{\ell jt}_{\pi N,\pi N}$ and $V^{\ell jt,L}_{\pi N,\gamma N}$ are real functions. Hence the quantity inside the square bracket of Eq. (4.10) is real. Therefore Eq. (4.10) shows that the phase of each pion photoproduction

multipole is identical to the πN scattering phase shift in the same eigenchannel. This is an explicit derivation of the Watson theorem[24] from a dynamical model. The form of Eq. (4.10) is identical to that given by Yang.[11]

We now emphasize an important feature of the Hamiltonian model. As seen in Eq. (4.10), the pion photoproduction amplitude contains a principal value (PV) term which depends on the πN off-shell interaction. When the (PV) term is neglected, the earlier approaches[5-9] using solely the Watson theorem to describe the final πN interaction is obtained from the present dynamical model. In Sec. V we will examine the dynamical consequence of this πN off-shell effect in interpreting the data.

Next we focus on the gauge invariance of the present model. The t-matrix Eq. (3.23a) in an arbitrary frame is written as

$$T_{\pi N,\gamma N}(kp',qp) = < \chi^{(-)}_{\vec{k},\vec{p}'} | j_\mu(0) | p > \epsilon^\mu(q,\lambda) \tag{4.12a}$$

where $< \chi^{(-)}_{\vec{k},\vec{p}'} |$ is the πN scattering state with pion momentum $\vec{k}$ and proton momentum $\vec{p}'$.

$$\begin{aligned}
&< \chi^{(-)}_{\vec{k},\vec{p}'} \mid j_\mu(0) \mid \vec{p} > \\
&= \int d\vec{k}'_{\pi N} \{\delta(\vec{k}'_{\pi N} - \vec{k}_{\pi N}) + T_{\pi N,\pi N}(\vec{k}_{\pi N}, \vec{k}'_{\pi N}, E) \frac{1}{E - E_N(\vec{k}'_{\pi N}) - E_\pi(\vec{k}'_{\pi N}) + i\epsilon}\} \\
&\quad [< \vec{k}' E_\pi(\vec{k}'), \vec{p}'' E_N(\vec{p}'') \mid J^{Born}_\mu(0) \mid \vec{p} E_N(\vec{p}) >] \\
&\qquad\qquad (2\pi)^3 F_{cut}(\vec{k}'_{\pi N}) F_\pi(\vec{k}') F_N(\vec{p}'') F_\gamma(\vec{q}) F_N(\vec{p}) \\
&\quad + f_{\pi N,\Delta}(\vec{k}_{\pi N}, E) \frac{1}{E - m_{0\Delta} - \Sigma_\Delta(E)} \\
&\quad [< \vec{p}_\Delta E_\Delta(\vec{p}_\Delta) \mid J^\Delta_\mu(0) \mid \vec{p} E_N(\vec{p}) >] (2\pi)^{3/2} F_\Delta(\vec{p}_\Delta) F_\gamma(\vec{q}) F_N(\vec{p}),
\end{aligned} \tag{4.12b}$$

where $\vec{k}'_{\pi N} = \frac{1}{2}(\vec{k}' - \vec{p}'')$, $\vec{k}_{\pi N} = \frac{1}{2}(\vec{k} - \vec{p}')$, and E is the total energy available in the πN c.m. system. The matrix elements of first and second brackets in Eq. (4.12b) are defined by Eqs. (2.8) and (2.9), respectively. The gauge invariance of the t-matrix Eq. (4.12a) is equivalent to the following current conservation.

$$< \chi^{(-)}_{\vec{k},\vec{p}'} \mid j_\mu(0) \mid \vec{p} > q^\mu \; = \; 0. \tag{4.13}$$

Eq. (4.13) is proved if the two square brackets of Eq. (4.12b) satisfy the current conservation separately for any values of momenta p, k', p'' and p_Δ. Namely,

$$< \vec{k}' E_\pi(\vec{k}'), \vec{p}'' E_N(\vec{p}'') \mid J^{Born}_\mu(0) \mid \vec{p} E_N(\vec{p}) > q^\mu = 0 \tag{4.14a}$$

$$< \vec{p}_\Delta E_\Delta(\vec{p}_\Delta) \mid J^\Delta_\mu(0) \mid \vec{p} E_N(\vec{p}) > q^\mu = 0. \tag{4.14b}$$

Using Eqs. (2.9b) and (2.10) Eq. (4.14b) becomes

$$\begin{aligned}
&< \vec{p}_\Delta E_\Delta(\vec{p}_\Delta) \mid J^\Delta_\mu(0) \mid \vec{p} E_N(\vec{p}) > q_\mu \\
&= ie_0(1/2,\tau,1,0 \mid 3/2,\tau_\Delta) \overline{w}^\mu(p_\Delta, s_\Delta) \Gamma_{\mu\nu} q^\nu u_N(p,s) \\
&= ie_0(1/2,\tau,1,0 \mid 3/2,\tau_\Delta) \overline{w}^\mu(p_\Delta, s_\Delta) \{G_M(q^2) K^M_{\mu\nu} q^\nu + G_E(q^2) K^E_{\mu\nu} q^\nu\} u_N(p,s) \\
&= 0.
\end{aligned} \tag{4.15}$$

The last line of the Eq. (4.15) is due to the use of the following identities

$$K^M_{\mu\nu} q^\nu = constant \cdot \epsilon_{\mu\nu\alpha\beta} q^\nu q^\beta P^\alpha = 0 \tag{4.16a}$$

$$K^E_{\mu\nu} q^\nu = -K^M_{\mu\nu} q^\nu + \epsilon_{\nu\lambda\gamma\delta} q^\nu p^\gamma_\Delta q^\delta X^\lambda_\mu = 0, \tag{4.16b}$$

where X^λ_μ is easily deduced from (2.10c). Therefore the Δ term is gauge invariant for any values of isospin projection and momenta p and p_Δ.

By using Eq. (2.8b), the Eq. (4.14a) leading to a charged $\pi^\pm$ final state can be explicitly written as

$$\begin{aligned}
&< \pi^\pm \vec{k}' E_\pi(\vec{k}'), \vec{p}'' E_N(\vec{p}'') \mid J^{Born}_\mu(0) \mid \vec{p} E_N(\vec{p}) > q_\mu \\
&= ie_0 \frac{f_{\pi NN}}{m_\pi} \overline{u}_N(p'',s'',\tau'') [\pm\tau_{\mp 1} \{-\gamma_5 \not{q} + \gamma_5 (\not{k}' - \not{q})(2k'\cdot q - q^2) \Delta_F(q-k')\} \\
&\quad + \{\tau_{\mp 1} \gamma_5 \not{k}' S_F(p+q) (\frac{1+\tau_3}{2}) \not{q} + (\frac{1+\tau_3}{2}) \not{q} S_F(p''-q) \gamma_5 \not{k}' \tau_{\mp 1}\}] u_N(p,s,\tau).
\end{aligned} \tag{4.17}$$

In Eq. (4.17) the γNN anomalous magnetic moment terms and vector meson term vanished because of the identities $\sigma_{\mu\nu} q^\mu q^\nu = 0$ and $\epsilon_{\mu\alpha\beta\gamma} q^\mu k'^\alpha q^\beta = 0$. We now recall that the momenta of all external legs (except the photon) are evaluated on their mass-shell. This means that we set $p^2 = p'^2 = m^2$ in evaluating the propagators in Eq. (4.17)

$$\Delta_F(q-k') = \frac{1}{(q-k')^2 - m^2_\pi} = \frac{1}{q^2 - 2k'\cdot q}, \tag{4.18a}$$

$$S_F(p+q) = \frac{\not{p} + \not{q} + m_N}{(p+q)^2 - m^2_N} = \frac{\not{p} + \not{q} + m_N}{q^2 + 2p\cdot q}, \tag{4.18b}$$

$$S_F(p''-q) = \frac{\not{p}'' - \not{q} + m_N}{(p''-q)^2 - m^2_N} = \frac{\not{p}'' - \not{q} + m_N}{q^2 - 2p''\cdot q}. \tag{4.18c}$$

Substituting Eqs. (4.18) into (4.17), we have

$$< \pi^{\pm}\vec{k}' E_\pi(\vec{k}'), \vec{p}'' E_N(\vec{p}'') \mid J_\mu^{Born}(0) \mid \vec{p} E_N(\vec{p}) > q_\mu$$

$$= ie_0 \frac{f_{\pi NN}}{m_\pi} \bar{u}_N(p'', s'', \tau'')[\pm\tau_{\mp 1}\{-\gamma_5 \not{q} + \gamma_5(\not{k}' - \not{q})(2k' \cdot q - q^2)\frac{1}{q^2 - 2k' \cdot q}\}$$

$$+\tau_{\mp 1}\gamma_5 \not{k}' \frac{(\not{p} + \not{q} + m_N)}{q^2 + 2p \cdot q}(\frac{1 + \tau_3}{2})\not{q} + (\frac{1 + \tau_3}{2})\not{q}\frac{(\not{p}'' - \not{q} + m_N)}{q^2 - 2p'' \cdot q}\gamma_5 \not{k}' \tau_{\mp 1}] u_N(p, s, \tau)$$

$$= ie_0 \frac{f_{\pi NN}}{m_\pi} \bar{u}_N(p'', s'', \tau'')[\mp\tau_{\mp 1}\gamma_5 \not{k}' + \tau_{\mp 1}(\frac{1 + \tau_3}{2})\gamma_5 \not{k}' \frac{(2p \cdot q - \not{q}\not{p} + q^2 + m_N \not{q})}{q^2 + 2p \cdot q}$$

$$+(\frac{1 + \tau_3}{2})\tau_{\mp 1}\frac{(2p'' \cdot q - \not{p}''\not{q} - q^2 + m_N \not{q})}{q^2 - 2p'' \cdot q}\gamma_5 \not{k}'] u_N(p, s, \tau). \tag{4.19}$$

Eq. (4.19) can be further simplified by using the Dirac equations $(\not{p} - m_N)u_N(p, s) = 0$ and $\bar{u}_N(p'', s'')(\not{p}'' - m_N) = 0$. We then have

$$< \pi^{\pm}\vec{k}' E_\pi(\vec{k}'), \vec{p}'' E_N(\vec{p}'') \mid J_\mu^{Born}(0) \mid \vec{p} E_N(\vec{p}) > q_\mu$$

$$= ie_0 \frac{f_{\pi NN}}{m_\pi} \bar{u}_N(p'', s'', \tau'')[\mp\tau_{\mp 1}\gamma_5 \not{k}' + \tau_{\mp 1}(\frac{1 + \tau_3}{2})\gamma_5 \not{k}' - (\frac{1 + \tau_3}{2})\tau_{\mp 1}\gamma_5 \not{k}'] u_N(p, s, \tau)$$

$$= ie_0 \frac{f_{\pi NN}}{m_\pi} \bar{u}_N(p'', s'', \tau'')\{\mp\tau_{\mp 1} + \frac{1}{2}[\tau_{\mp 1}, \tau_3]\}\gamma_5 \not{k}' u_N(p, s, \tau)$$

$$= 0. \tag{4.20}$$

The proof for π^0 production is very similar. Using Eqs. (2.8c) and (4.18), we have

$$< \pi^0\vec{k}' E_\pi(\vec{k}'), \vec{p}'' E_N(\vec{p}'') \mid J_\mu^{Born}(0) \mid \vec{p} E_N(\vec{p}) > q_\mu$$

$$= -ie_0 \frac{f_{\pi NN}}{m_\pi} \bar{u}_N(p'', s'', \tau'')[\tau_3 \gamma_5 \not{k}' S_F(p + q)(\frac{1 + \tau_3}{2})\not{q}$$

$$+(\frac{1 + \tau_3}{2})\not{q} S_F(p'' - q)\gamma_5 \not{k}' \tau_3] u_N(p, s, \tau)$$

$$= -ie_0 \frac{f_{\pi NN}}{m_\pi} \bar{u}_N(p'', s'', \tau'')(\frac{1 + \tau_3}{2})\{\gamma_5 \not{k}' \frac{(\not{p} + \not{q} + m_N)}{q^2 + 2p \cdot q}\not{q}$$

$$+\not{q}\frac{(\not{p}'' - \not{q} + m_N)}{q^2 - 2p'' \cdot q}\gamma_5 \not{k}'\} u_N(p, s, \tau)$$

$$= -ie_0 \frac{f_{\pi NN}}{m_\pi} \bar{u}_N(p'', s'', \tau'')(\frac{1 + \tau_3}{2})\{\gamma_5 \not{k}' \frac{(2p \cdot q - \not{q}\not{p} + q^2 + m_N \not{q})}{q^2 + 2p \cdot q}$$

$$+\frac{(2p'' \cdot q - \not{p}''\not{q} - q^2 + m_N \not{q})}{q^2 - 2p'' \cdot q}\gamma_5 \not{k}'\} u_N(p, s, \tau)$$

$$= -ie_0 \frac{f_{\pi NN}}{m_\pi} \bar{u}_N(p'', s'', \tau'')(\frac{1 + \tau_3}{2})\{\gamma_5 \not{k}' - \gamma_5 \not{k}'\} u_N(p, s, \tau)$$

$$= 0. \tag{4.21}$$

This completes the proof of the gauge invariance of our formulation.

Before we end this section, two remarks should be made. First, in the derivations of the Eqs. (4.15), (4.20) and (4.21), no restriction was made for the photon momentum; i.e. q^2 can be either zero for a real photon or non-zero for a virtual photon. Therefore the model presented here can be directly used to carry out a gauge invariant calculation of electroproduction of pions on the nucleon (provided that we assign the isovector γNN form factor $F_1^V(q^2)$ to diagrams Figs. 1(c) and 1(d)).[28] Second, the momentum variables of the propagators in the Born terms, Figs. 1(a)-1(d), can be calculated using either the initial γN momenta or the final πN momenta. For example, within the Feynman rules it is legitimate to specify the intermediate nucleon momentum of Fig. 1(a) as $p''+k'$ instead of $p+q$ as used in Eq. (4.18b) and the subsequent derivations. Similarly, we can specify the intermediate nucleon momentum of Fig. 1(b) as $p-k'$ instead of the $p''-q$ used in Eq. (4.18c). These different choices are equivalent on-energy-shell. However in our three-dimensional formulation they are not equivalent, since the calculation involves off-energy-shell matrix elements, as seen in Eq. (4.12b). The proofs given in Eqs. (4.19)-(4.21) come about only when the choices given in Eqs. (4.18) are made. Our finding is obtained only by inspection. Perhaps this choice is unique, but further investigation is needed.

V. Results and Discussions

The first step of our study is to determine the hadronic Hamiltonian H_I of Eq. (3.2c). The parametrizations of the bare vertex interactions $f^0_{\pi N,B}$ (with $B = \Delta, N$), and the two-body potential $v_{\pi N,\pi N}$, are given in Appendix A. The solution of the πN scattering equations (3.8)-(3.12) is also given explicitly there. In Fig. 2 the fits to the partial wave πN phase shifts are presented, with the corresponding parameters being given in Table 2. Here we only mention that two different P_{33} models have been constructed. Their main difference is in the parametrization of the $\pi N \leftrightarrow \Delta$ vertex. The first one, given in Eq. (A.4b), is a typical modified Yamaguchi form. Its fit to the P_{33} phase shift is displayed in Fig. 2, along with the results for other partial waves. The second one is based on the cloudy bag model[23] parametrization, Eq. (3.14). Three models with bag radii $R = 0.8, 1.0, 1.2$ fm have been constructed. The resulting parameters are given in Table 3. Their fits to the P_{33} phase shift are almost indistinguishable from that given in Fig. 2, and therefore will not be given separately. These three models allow us to examine model dependence in our study of the Δ excitation. No attempt is made to relate the P_{11} parameters to the cloudy bag model, since its dynamical content is much more complicated and less understood.

The equations for pion photoproduction, Eqs. (3.22), are solved without employing the usual partial wave decomposition. This greatly simplifies the needed analytical work. The price we pay is in having to develop an efficient numerical method for calculating the current matrix elements, given in Sec. II, which contain complicated Dirac algebra. The three dimensional integration needed to calculate the contribution of the πN final state interaction (FSI), is carried out by using the standard method of contour rotation to handle the singularity of the πN propagator. The calculation of multipole amplitudes is discussed in Appendix B, while the conventions for cross sections and polarization observables are presented in Appendix C.

For the following discussion, it will be useful to introduce some nomenclature for the various contributions to the photoproduction amplitude of Eqs. (3.22). We shall refer to the contribution from $v^{Born}_{\pi N,\gamma N}$ alone as the *Born* term. The total contribution from $v^{Born}_{\pi N,\gamma N}$ including the πN final state interaction will be called the *nonresonant* term. The Δ term refers to the contribution from the resonant term in Eqs. (3.22). The calculation neglecting the principal value part of the πN propagator, i.e. neglecting the (PV) term in Eq. (4.10), will be called the *on-shell-unitary* approach. Apart form the $cos\delta^{jt}_\ell$ factor in Eq. (4.10), such an approach is equivalent to just using the Watson theorem to describe the πN final state interaction. The $cos\delta^{jt}_\ell$ factor gives an energy dependent scale factor for the summed Born and Δ terms, and might effectively be included even in the simplest models of photoproduction through phenomenological coupling constants.

Once the hadronic Hamiltonian H_S is determined, our model has only three independent parameters: the range Λ of the Born term cutoff form factor Eq. (3.19b), and the strengths $G_M(\equiv G_M(0))$ and $G_E(\equiv G_E(0))$ defined in Eq. (2.10a). Our strategy is to first determine these three parameters by fitting the existing $M_{1+}(3/2)$ and $E_{1+}(3/2)$ multipole amplitudes. Then the validity of the model is determined by comparing the predicted cross sections and polarization observables with experimental data.[32] Although other multipole amplitudes will be compared with the analyses of Refs. 33 and 34, we will place less significance on this comparison, since the multipole analyses themselves are model dependent.

Fig. 3 shows fits to the $M_{1+}(3/2)$ and $E_{1+}(3/2)$ multipoles obtained by using the P_{33} model with a bag radius $R = 1.0$ fm. The resulting parameters are G_M=2.28, G_E=0.07 and Λ=650 MeV/c. Also displayed are the contributions from the nonresonant term (dash curves). It is seen that the nonresonant term plays an important role in describing the data. Its contributions to the imaginary parts are of course only due to the FSI term of Eq. (3.22a), since the Born term alone is a real quantity. To see the model dependence, we have tried to fit the multipoles using the other two P_{33} models with bag radii $R = 0.8$ and 1.2 fm. The resulting fits are comparable to that shown in Fig. 3, and the existing data cannot distinguish between them. The corresponding values of G_M and G_E are within 5% of the values of the $R = 1.0$ fm model. The required values of Λ are also about 650 MeV/c; however, no good fit can be achieved with $\Lambda < 500$ MeV/c or $\Lambda > 750$ MeV/c. This will be confirmed later when we examine the dependence of the predicted cross sections on the value of Λ. We conclude that the model dependence of the extracted Δ parameters G_M and G_E is about 5%. We will use the model with a radius $R = 1.0$ fm for the rest of the calculations.

One of the most quoted parameters for the $\Delta \leftrightarrow \gamma N$ transition is the $E2/M1$ ratio R_{EM} (its precise definition is discussed in Appendix B). Our values of $G_M = 2.28$ and $G_E = 0.07$ yield $R_{EM} = -G_E/G_M = -3.1\%$. Several authors have proposed different numbers for R_{EM}: For example, -1.5% by Davidson, Mukhopadhyay and Wittman,[6] $+3.7\%$ by Tanabe and Ohta[10] and -7.9% by Yang,[11] where the number -7.9% by Yang is obtained using $G_M = 5.3$ and $G_E = 0.42$ of Ref. 11. In Appendix B we show the relation between two different coupling schemes so that coupling constants can be directly compared. The differences between the present values and the nonrelativistic quark model's predictions $G_M = 2.62$ and $G_E = 0$, point to the need for a detailed theoretical understanding of the mesonic structure of the nucleon.

In Figs. 4-6, the predicted differential cross sections for pion photoproduction are compared with the experimental data.[32] In Fig. 7 we also compare the predicted results with the most recent $\gamma n \to \pi^- p$ data[35] from TRIUMF. The total cross sections are displayed in Figs. 8. Overall agreement with the data is quite

good. However, in the high energy region our model only gives a qualitative description of the data. The model also has problems in describing the π^0 data in the low energy region. Later we will explore this problem in more detail.

Before we proceed further, it should be mentioned that the results displayed in Figs. 3-8 show a substantial improvement over the early, but widely used non-unitary model of Laget.[8,9] As pointed out later in Ref. 9, the neglect of unitarity is especially bad for π^0 production. We further note that the same set of the parameters, listed in Table 1, is used in our calculations for all the three charged pion channels, $\gamma n \to \pi^- p$, $\gamma p \to \pi^+ n$ and $\gamma p \to \pi^0 p$. In contrast, different parameters are used in Ref. 9 for π^0 and $\pi^\pm$ production, implying a large charge dependence in the basic coupling constants.

We now turn to reveal several important dynamical features of the present Hamiltonian approach. First we note from Fig. 3 that the nonresonant term is as important as the Δ term in determining the pion photoproduction cross section in the entire energy region. It is therefore important to examine the extent to which our results depend on the only free parameter in the calculation of the nonresonant term: the range Λ for the cutoff form factor of Eq. (3.19b). We have performed three calculations: with Λ=350, 650 and 900 MeV/c. For each value of Λ, the values of G_M and G_E are chosen appropriately so that the fits to the $M_{1+}(3/2)$ and $E_{1+}(3/2)$ multipole amplitudes compare favourably to what has been given in Fig. 3. The resulting predictions for differential cross sections are shown in Fig. 9. It is clear that the calculated cross sections depend strongly on the chosen value of Λ. Overall, the choice Λ=650 MeV/c gives the best results. If we naively relate the value of Λ to the range of the photo-meson interaction by a relation $r = \sqrt{6}/\Lambda$, then we find that our best fit requires r=0.74 fm. This is close to the radii of the nucleon and the Δ used in most of the cloudy bag model studies of baryon structure. Of course Λ is a phenomenological parameter in the present model, and can be interpreted as a hadron radius only qualitatively.

The importance of unitarity in pion photoproduction can be illustrated particularly well by its effect on the multipoles $M_{1+}(3/2)$ and $E_{1+}(3/2)$. If we leave out the FSI from our nonresonant term and set $\Lambda = \infty$ in the Born term, we essentially obtain Laget's original model.[9] This is illustrated in Fig. 10. The Born term contributions (dashed curves) are real and structureless. The total contribution (solid curves) gives a very poor fit to the multipoles, and is very similar to that obtained by Laget.[9] By varying the values of G_M and G_E within reasonable ranges, we have found that it is impossible to fit the multipoles with the non-unitary model. Comparing the dashed curves of Figs. 3 and 10, the problem with a non-unitary calculation is evidently a lack of an oscillating energy dependence.

We now turn to the differences between our model and the earlier unitary models[4-7] using solely the Watson theorem to describe the FSI. As discussed in Sec. IV, our model satisfies the off-shell unitarity relation Eq. (4.7), which for

on-shell kinematics is equivalent to Watson's theorem. The main consequence of our dynamical treatment of the FSI is in the appearance of the (PV) term in Eq. (4.10). It arises from an integration over the half-off-shell R-matrix. We therefore shall call those earlier unitary models the ***on-shell-unitary*** models. It is clear that the πN wave function at short distances is relevant in our approach, while the on-shell-unitary models essentially assume a free wave function even in the interaction region. The importance of this wave function effect is of course model dependent. Within the present model, we find that it accounts for as much as half of the calculated cross sections. This is shown in Fig. 11. In Fig. 12 we also see that when the (PV) term is set to zero (dashed curves), the resulting $M_{1+}(3/2)$ amplitude is significantly different from that of the full calculation (solid curves). This means that if the on-shell-unitary approach is used in our fit to these multipoles, the resulting R_{EM} will be very different from what we have obtained. As an example, we show in Fig. 13, that our on-shell-unitary calculation can also fit the $M_{1+}(3/2)$ and $E_{1+}(3/2)$ amplitudes, but with very different values of the Δ parameters G_M= 3.2 and G_E=0.0 . Perhaps this is the reason why the value $R_{EM} = -1.5\%$, obtained by Davidson et.al,[6] is rather different from our value -3.1%.

Now we examine the vector meson (ρ and ω) contribution to the differential cross sections. As one can see from Table 1, ρNN and $\rho\gamma\pi$ coupling constants are a factor three smaller than the corresponding coupling constants for ωNN and $\omega\gamma\pi$. Thus the ρ exchange contribution is much smaller than the ω exchange contribution. The most disappointing result in Figs. 4-6 is that of the differential cross sections for π^0 production in the low energy region. The main difference between π^0 and $\pi^\pm$ production is the contribution of the ω exchange diagram (Fig. 1(f)) to the Born term. To explore the importance of the ω exchange diagram, we have carried out calculations setting the ρ and ω exchange terms to zero. The $M_{1+}(3/2)$ and $E_{1+}(3/2)$ amplitudes can be fitted by setting $G_M = 2.4$ and $G_E = 0.07$ with Λ=650 MeV/c. The quality of the fit is as good as that shown in Fig. 3. The predicted differential cross sections are the dashed curves in Fig. 14. Comparing these results (dashed curves) with the results including vector meson exchange diagrams (solid curves), it is clear that the ω exchange diagram is essential to describe the differential cross sections of π^0 production at higher energy region. The ω exchange term is also responsible for getting better results in the low energy region, but it is clearly not sufficient. The present model is therefore not able to resolve the longstanding problem of π^0 photoproduction at threshold.[36] Clearly new mechanisms have to be discovered in the future. The vector meson exchange contribution is small in $\pi^\pm$ production, since the ω exchange diagram does not contribute and the ρ-exchange contribution is very weak.

To further explore the role of vector meson exchange, in Fig. 15 we compare all

s- and p-wave multipole amplitudes calculated with (solid curves) and without (dashed curves) the vector meson exchange diagrams. The data are from the analysis of Refs. 33 and 34. We see that the vector meson exchange significantly improves the fits to the E_{0+}, M_{1+} and M_{1-} multipoles. Note that the ρ exchange term markedly improves the $E_{0+}(0)$ amplitude, where ω exchange contribution is zero. However, the vector meson exchange effect is not sufficient to improve the fits to the $M_{1-}(1/2)$ multipole. As pointed out by Olsson and Osypowski,[5] this problem can be resolved by including the crossed Δ diagram which is not included in the present calculation within the subspace $S = \pi N \bigoplus B$ with $B = N, \Delta$. Such a calculation can be carried out consistently only when we extend the formulation to include the coupling to a $\pi\Delta$ channel. Such a πN model has been developed in Ref. 31, and the calculation can be done in the near future.

To end this section, we compare our predictions of various polarization observables with the data. These are expected to contain more detailed information about the underlying dynamics. The results for γ-asymmetry, target asymmetry and recoil nucleon asymmetry are presented in Figs. 16, 17 and 18, respectively. Their definitions are given by Eqs. (C.10)-(C.12). Overall agreement is very good. Our model agrees especially well with the γ-asymmetry data, where a large amount of data is available. On the other hand, for the other two asymmetries the amount of data is both limited and of relatively low accuracy. Clearly there is a need for further improvement in the polarization data - especially for the target asymmetry and the recoil nucleon asymmetry. These results together with the ones shown in Figs. 4-8 indicate that our model is a reasonable starting point for investigating pion photoproduction in the two- and many-nucleon systems - the objective (4) listed in the beginning of the paper.

VI. Summary

We have proposed a dynamical model of pion photoproduction on the nucleon. Based on a model Hamiltonian, the input interactions consist of bare vertices $f^0_{\pi N\Delta}$ and $f^0_{\gamma N\Delta}$, as well as potentials $v_{\pi N,\pi N}$ and $v^{Born}_{\pi N,\gamma N}$ for πN elastic scattering and pion photoproduction, respectively. The vertex $f^0_{\pi N\Delta}$ was taken to be that of the cloudy bag model, while the potential $v_{\pi N,\pi N}$ was assumed to be separable in each partial wave. To specify $f^0_{\gamma N\Delta}$ and $v^{Born}_{\pi N,\gamma N}$, we started from a relativistic Lagrangian, and reduction to three dimensions was achieved by (i) putting all particles on their mass shell, and (ii) choosing off-energy-shell momenta in such a way as to preserve gauge invariance.

Our resulting model has the following features: (1) It is unitary and gauge invariant. (2) It treats the final state πN interaction dynamically, with all s-, p- and d-wave πN phase shifts being well reproduced below 500 MeV. (3) It relates the electromagnetic excitation of the Δ resonance to the chiral/cloudy bag model of hadron structure. (4) For photon energies below 500 MeV, it describes the bulk of the available pion photoproduction data very well.

Once the πN interaction is determined, the model has only three free parameters: Λ, G_M and G_E, which are the cutoff momentum for the Born term and the electromagnetic form factors of $f^0_{\gamma N\Delta}$, respectively. By fitting $M_{1+}(3/2)$ and $E_{1+}(3/2)$ multipole data (Fig. 3), we have obtained Λ=650 MeV/c, G_M=2.28 and G_E=0.07. This results in a value for the E2/M1 ratio of -3.1%.

The model has been applied to carry out extensive calculations of cross sections and various spin observables. Most results are in very good agreement with the data (Figs. 4-8 and Figs. 16-18), and in general our results appear to be a substantial improvement over existing models. However, a major difficulty persists in describing the π^0 production in the low energy region (below 250 MeV incident photon energy). We find that the addition of vector meson (ρ and ω) exchange does not resolve this problem. We therefore conclude, that some new mechanism is needed to describe satisfactorily the π^0 production.

The dynamical content of the model has been explored in detail. It is shown that the calculated cross sections depend strongly on the cutoff parameter Λ. The best description of *all* data requires Λ= 650 MeV/c, which is consistent with the radii of the nucleon and the Δ within the cloudy bag model.

The importance of unitarity in determining the photoproduction mechanisms has also been studied. It is shown that if unitarity is neglected, as was done in a previous work,[8] the extracted values of G_M and G_E of the Δ excitation are significantly different from that of the present unitary model. We have also shown that in a Hamiltonian formulation of a unitary model, the pion photoproduction amplitude necessarily contains a part determined by the πN off-shell t-matrix. Within the present model, as much as half of the differential cross

section magnitude (Fig. 11) is due to this off-shell effect; i.e the πN wavefunction is strongly distorted and cannot be approximated by a plane wave. This off-shell effect is not included in those models that impose unitarity by appealing to Watson's theorem (which only uses the πN phase shifts to describe the final state interaction). This difference with the present model leads to very different interpretations of the data in terms of fundamental parameters, such as G_M and G_E of the Δ excitation.

Finally, the predicted multipole amplitudes have been compared with the multipole analysis data (Fig. 15). We have found that the description of final state interactions, provided by the present unitary calculation, leads to a satisfactory description of imaginary parts of multipole amplitudes in most channels.

To end, we would like to mention some possible future developments. One feature of our model is that it is consistent with the existing unitary descriptions of the πNN system. Our formalism can therefore be applied directly to calculate the electromagnetic production of pions on the deuteron. By treating the nucleon and Δ on the same footing, it should also be straightforward to extended the model to include $\pi\Delta$ states. This would enable a study of photoproduction at energies higher than 500 MeV incident photon energy. The needed πN model including coupling to the $\pi\Delta$ channel, has been constructed by Blankleider and Walker.[31] The present approach of calculating the final state interaction is also applicable to the study of pion weak-production on a nucleon; e.g. $\nu_\mu + N \to \mu^- + \pi + N'$. This may lead to a better understanding of the $N \leftrightarrow \Delta$ axial vector transitions. Perhaps the most straightforward application of the present model is to pion electroproduction on the nucleon ($eN \to e'\pi N$). Because electroproduction takes place via an off-shell photon, one can study the electromagnetic form factors at non-zero values of q^2. This study is now in progress.

Acknowledgements

The authors would like to thank Prof. N. Mukhopadhyay and Dr. R. Wittman for their useful discussions and for providing us with a part of their numerical code. One of us (B.B.) is indebted to Dr. J. T. Londergan for many fruitful discussions. This work was supported in part by the National Sciences and Engineering Research Council of Canada.

References

[1]G. F. Chew, M. L. Goldberger, F. E. Low and Y. Nambu, Phys. Rev. **106**, 1345 (1957).
[2]F. A. Berends, A. Donnachie and D. L. Weaver, Nucl. Phys. **B4**, 1 (1967), *ibid.* **B4**, 54 (1967) and *ibid.* **B4**, 103 (1967).
[3]See the review by A. Donnachie, High Energy Physics Vol.V, page 1, edited by E. Burhop, Academic Press New York 1972.
[4]R. D. Peccei, Phys. Rev. **181**, 1902 (1969).
[5]M. G. Olsson, Nucl. Phys. **B78**, 55 (1974); M. G. Olsson and E. T. Osypowski, Nucl. Phys. **B87**, 399 (1975); Phys. Rev. **D17**, 174 (1978).
[6]R. Wittman, R. Davidson and N. C. Mukhopadhyay, Phys. Lett. **142B**, 336 (1984); R. Davidson, N. Mukhopadhyay and R. Wittman, Phys. Rev. Lett. **56**, 804 (1986).
[7]J. L. Sabutis, Phys. Rev. **C27**, 778 (1983).
[8]I. Blomquist and J. M. Laget, Nucl. Phys. **A280**, 405 (1977).
[9]J. M. Laget, Phys. Rep. **69**, 1 (1981)
[10]H. Tanabe and K. Ohta, Phys. Rev. **C31**, 1876 (1985).
[11]S. N. Yang, J. Phys. **G11**, L205 (1985); a very similar calculation was performed by Zhang Xi-zhen, Chen Bao-qiu, Chen Hua-zhong, Han Wen-shu and Jin Xing-nan, to be published in Chinese Nuclear Physics.
[12]L. Heller, S. Kumano, J. C. Martinez and E. J. Moniz, Phys. Rev. **C35**, 718 (1987).
[13]S. Kumano, Phys. Lett. **B214**, 132 (1988); Nucl. Phys. **A**, to be published.
[14]G. Kälberman and J. M. Eisenberg, Phys. Rev. **D28**, 71 (1983); **D29**, 517 (1984).
[15]M. Weyrauch, Phys. Rev. **D35**, 1574 (1987).
[16]S. Scherer, D. Drechsel and L. Tiator, Phys. Lett. **B193**, 1 (1987).
[17]M. Araki and I. R. Afnan, Phys. Rev. **C36**, 250 (1987).
[18]I. R. Afnan and B. Blankleider, Phys. Rev. **C22**, 1638 (1980); **C24**, 1572 (1981); **C32**, 2006 (1985).
[19]A.W. Thomas and A. S. Rinat, Phys. Rev. **C20**, 216 (1979); A. S. Rinat and Y. Starkand, Nucl. Phys. **A397**, 381 (1983); A. S. Rinat and R. S. Bhalerao, Weizmann Institute of Science Report, WIS-82/55 Nov-Ph, 1982.
[20]Y. Avishai and T. Mizutani, Nucl. Phys. **A326**, 352 (1979); **A338**, 377 (1980); **A352**, 399 (1981); Phys. Rev. **C27**, 312 (1983); C. Fayard, G. H. Lamot, and T. Mizutani, Phys. Rev. Lett. **45**, 524 (1980); G. H. Lamot, J. L. Perrot, C. Fayard, and T. Mizutani, Phys. Rev. **C35**, 239 (1987).
[21]H. Pöpping, P. U. Sauer, and Zhang Xi-Zhen, Nucl. Phys. **A474**, 557 (1987).
[22]M. Betz and T.-S. H. Lee, Phys. Rev. **C23**, 375 (1981); T.-S. H. Lee and A. Matsuyama, Phys. Rev. **C32**, 516 (1985); **C32**, 1986 (1985); **C34**, 1900 (1986).

[23]A. W. Thomas, Advances in Nuclear Physics Vol.13, page 1, edited by J. W. Negele and E. Vogt, Plenum Press 1984, and references are cited therein.
[24]K. M. Watson, Phys. Rev. **95**, 228 (1954).
[25]H. F. Jones and M. D. Scadron, Ann. of Phys. **81**, 1 (1973).
[26]J. D. Bjorken and S. D. Drell, *Relativistic Quantum Mechanics*, (McGraw-Hill, New York 1964).
[27]D. M. Brink and G. R. Satchler, *Angular Momentum*, (Clarendon Press, London 1968).
[28]E. Amaldi, S. Fubini and G. Furlan, *Pion-Electroproduction*, Springer Tracts in Modern Physics **83**, (Springer Verlag, Berlin 1979).
[29]I. R. Afnan and A. T. Stelbovics, Phys. Rev. **C23**, 1384 (1981).
[30]M. L. Goldberger and K. M. Watson, *Collision Theory*, (John Wiley and Sons, New York, 1964).
[31]B. Blankleider and G. E. Walker, Phys. Letts. **152B**, 291 (1985).
[32]D. Menze, W. Pfeil and R. Wilcke, ZAED Compilation of Pion Photoproduction Data, University of Bonn 1977.
[33]F. A. Berends and A. Donnachie, Nucl. Phys. **B84**, 342 (1975).
[34]W. Pfeil and D. Schwela, Nucl. Phys. **B45**, 379 (1972).
[35]A. Bagheri, K.A. Aniol, F. Entezami, M.D. Hasinoff, D.F. Measday, J-M. Poutissou, M. Salomon and B. C. Robertson, Phys. Rev. **C38**, 875 (1988).
[36]E. Mazzucato *et al.* Phys. Rev. Lett. **57**, 3144 (1986).
[37]G. Höhler, F. Kaiser, R. Koch and E. Pietarinen, *Handbook of Pion-Nucleon Scattering*, Physics Data 12-1, Karlsruhe, 1979.

APPENDIX

A. πN separable form factors

Within the formalism of our Hamiltonian model, presented in Sec. III, the equation describing πN scattering is given by Eq. (3.6a). For a partial wave specified by quantum numbers ℓjt, this equation takes the form

$$T^{\ell jt}_{\pi N,\pi N}(k_f,k_i,E) = V^{\ell jt}_{\pi N,\pi N}(k_f,k_i,E) + \int dk k^2 V^{\ell jt}_{\pi N,\pi N}(k_f,k,E) G_{\pi N}(k,E) T^{\ell jt}_{\pi N,\pi N}(k,k_i,E), \qquad (A.1)$$

with

$$G_{\pi N}(k,E) = \frac{1}{E - E_\pi(k) - E_N(k) + i\epsilon}, \qquad (A.2a)$$

where k and E are, respectively, the πN relative momentum and the total collision energy in the center of mass frame. For our calculations we use relativistic kinematics for both pion and nucleon, thus

$$E_\pi(k) = (k^2 + m_\pi^2)^{1/2}, \qquad (A.2b)$$

$$E_N(k) = (k^2 + m_N^2)^{1/2}. \qquad (A.2c)$$

As shown by Eq. (3.6b), the energy dependent πN potential $V^{\ell jt}_{\pi N,\pi N}(k,k',E)$ is due to both the vertex interaction $f^0_{\pi N,B}$, and the "background" potential $v_{\pi N,\pi N}$ which in the present paper is assumed to be of a separable form. The on-shell value of the t-matrix is related to the phase shift by Eq. (C.6). Parameters of the potential are determined by fitting the phase shift data[37] up to 500 MeV pion laboratory kinetic energy. In the following presentation, we drop the indices ℓjt for simplicity.

i) P_{11} and P_{33} channels

For P_{11} and P_{33} channels, both terms on the right hand side of Eq. (3.6b) can contribute. Thus the total potential matrix element can be written in terms of (baryon) pole and non-pole parts:

$$V_{\pi N,\pi N}(k_f,k_i,E) = f_0(k_f) g^0_B(E) f_0(k_i) + h_0(k_f)\lambda_0 h_0(k_i), \qquad (A.3)$$

where λ_0 ($= \pm 1$) is a phase parameter and $g^0_B(E) = 1/(E - m_{0B})$. The form factors $h_0(k)$ and $f_0(k)$ are parameterized as follows

$$h_0(k) = \frac{a_1 k^{m_1}}{(k^2 + b_1^2)^{n_1}} k^\ell, \qquad (A.4a)$$

$$f_0(k) = \frac{a_2 k^{m_2}}{(k^2+b_2^2)^{n_2}} k^\ell. \qquad (A.4b)$$

The values of the parameters are given in Table 2. The resulting fits to the πN phase shift data are displayed in Fig. 2. We also have constructed three P_{33} models based on the cloudy bag model parameterization Eq. (3.14). The resulting parameters are given in Table 3. Their fits to the πN phase shift data are indistinguishable from that shown in Fig. 2.

By inserting Eq. (A.3) into Eq. (A.1), the πN amplitude can be written as

$$T_{\pi N,\pi N}(k_f,k_i,E) = T^{NP}_{\pi N,\pi N}(k_f,k_i,E) + f(k_f)g_B(E)f(k_i), \qquad (A.5)$$

where the non-pole t-matrix is given by

$$T^{NP}_{\pi N,\pi N}(k_f,k_i,E) = h_0(k_f)\tau_0(E)h_0(k_i), \qquad (A.6)$$

$$\tau_0(E) = \frac{\lambda_0}{1-\lambda_0 \int dk k^2 \mid h_0(k) \mid^2 G_{\pi N}(k,E)}. \qquad (A.7)$$

The pole term in Eq. (A.5) consists of a dressed form factor $f(k_\alpha)$ ($\alpha = i, f$) and a dressed propagator $g_B(E)$ defined by

$$f(k_\alpha) = f_0(k_\alpha) + \tau_0(E)h_0(k_\alpha)\int dk k^2 h_0(k) f_0(k) G_{\pi N}(k,E), \qquad (A.8)$$

$$g_B(E) = \frac{1}{E - m_{0B} - \int dk k^2 f^*(k) f_0(k) G_{\pi N}(k,E)}. \qquad (A.9)$$

ii) other πN channels

For channels other than P_{11} and P_{33}, the vertex interaction of Eq. (3.6b) does not contribute. The πN potential is then assumed to be of rank-2 separable form

$$v_{\pi N,\pi N}(k_f,k_i) = h_1(k_f)\lambda_1 h_1(k_i) + h_2(k_f)\lambda_2 h_2(k_i). \qquad (A.10)$$

The form factors are parameterized as

$$h_1(k) = \frac{a_1 k^{m_1}}{(k^2+b_1^2)^{n_1}} k^\ell, \qquad (A.11a)$$

$$h_2(k) = \frac{a_2 k^{m_2}}{(k^2+b_2^2)^{n_2}} k^\ell. \qquad (A.11b)$$

As before, the parameters in each partial wave may be found in Table 2, with the resulting fits to the πN phase shift data being given in Fig. 2.

By inserting Eq. (A.10) into Eq. (A.1), one obtains the following analytic solution

$$T_{\pi N,\pi N}(k_f,k_i,E) = h_1(k_f)\tau_{11}(E)h_1(k_i) + h_1(k_f)\tau_{12}(E)h_2(k_i)$$

$$+h_2(k_f)\tau_{21}(E)h_1(k_i) + h_2(k_f)\tau_{22}(E)h_2(k_i), \qquad (A.12)$$

where

$$\tau_{11}(E) = \frac{\lambda_1(1-\lambda_2 H_2)}{(1-\lambda_1 H_1)(1-\lambda_2 H_2) - \lambda_1\lambda_2 H_{12}^2}, \qquad (A.13a)$$

$$\tau_{12}(E) = \tau_{21}(E) = \frac{\lambda_1\lambda_2 H_{12}}{(1-\lambda_1 H_1)(1-\lambda_2 H_2) - \lambda_1\lambda_2 H_{12}^2}, \qquad (A.13b)$$

$$\tau_{22}(E) = \frac{\lambda_2(1-\lambda_1 H_1)}{(1-\lambda_1 H_1)(1-\lambda_2 H_2) - \lambda_1\lambda_2 H_{12}^2}, \qquad (A.13c)$$

and

$$H_1 = \int dk k^2 \mid h_1(k) \mid^2 G_{\pi N}(k,E), \qquad (A.14a)$$

$$H_2 = \int dk k^2 \mid h_2(k) \mid^2 G_{\pi N}(k,E), \qquad (A.14b)$$

$$H_{12} = \int dk k^2 h_1(k) h_2(k) G_{\pi N}(k,E). \qquad (A.14c)$$

B. Multipole amplitudes and Definition of R_{EM}

Following the standard CGLN convention,[1] the multipole amplitudes for each charge state α can be calculated from the following equations

$$\begin{pmatrix} E^\alpha_{l+} \\ E^\alpha_{l-} \\ M^\alpha_{l+} \\ M^\alpha_{l-} \end{pmatrix} = \int_{-1}^{+1} dx\, D_l(x) \begin{pmatrix} J^\alpha_1 \\ J^\alpha_2 \\ J^\alpha_3 \\ J^\alpha_4 \end{pmatrix}, \qquad (B.1)$$

where $x = \hat{q}\cdot\hat{k}$. Here $\hat{q}$ and $\hat{k}$ are unit vectors of photon and pion, respectively. The 4×4 matrix $D_l(x)$ is defined as

$$D_l(x) = \begin{pmatrix} \frac{1}{2(l+1)}[& P_l & -P_{l+1} & \frac{l}{2l+1}(P_{l-1}-P_{l+1}) & \frac{l+1}{2l+3}(P_l-P_{l+2}) &] \\ \frac{1}{2l}[& P_l & -P_{l-1} & \frac{l+1}{2l+1}(P_{l+1}-P_{l-1}) & \frac{l}{2l-1}(P_l-P_{l-2}) &] \\ \frac{1}{2(l+1)}[& P_l & -P_{l+1} & \frac{1}{2l+1}(P_{l+1}-P_{l-1}) & 0 &] \\ \frac{1}{2l}[& -P_l & P_{l-1} & \frac{1}{2l+1}(P_{l-1}-P_{l+1}) & 0 &] \end{pmatrix}, \qquad (B.2)$$

where $P_l \equiv P_l(x)$ is the Legendre polynomial. The invariant amplitudes J^α_i ($i = 1,2,3,4$) are related to $M^\alpha_{\pi N,\gamma N}$ (Eq. (C.1)) in the c.m. frame ($\vec{p} = -\vec{q}$, $\vec{p}\,' = -\vec{k}$) by

$$M^\alpha_{\pi N,\gamma N} = \frac{4\pi E}{m_N} \chi^\dagger_{s'} J^\alpha \chi_s \qquad (B.3)$$

with

$$J^\alpha = i\vec{\sigma}\cdot\vec{\epsilon}(q,\lambda)J_1^\alpha + \vec{\sigma}\cdot\hat{q}\vec{\sigma}\cdot(\hat{k}\times\vec{\epsilon}(q,\lambda))J_2^\alpha + i\vec{\sigma}\cdot\hat{k}\hat{q}\cdot\vec{\epsilon}(q,\lambda)J_3^\alpha + i\vec{\sigma}\cdot\hat{q}\hat{q}\cdot\vec{\epsilon}(q,\lambda)J_4^\alpha, \tag{B.4}$$

where E is the center of mass energy of the πN system and $\chi_s(\chi_{s'}^\dagger)$ specifies the z-component of the initial(final) nucleon spin. In turn, the invariant amplitude $M^\alpha_{\pi N,\gamma N}$ is related to the t-matrix $T^\alpha_{\pi N,\gamma N}$ of Eq. (3.23) by relation Eq. (C.4).

The calculations of multipole amplitudes are carried out by the following procedure. First the matrix elements of the pion photoproduction amplitude $T^\alpha_{\pi N,\gamma N}$(Eq. (3.23)) are calculated by carrying out three-dimension integrations over the intermediate πN momentum. For each allowed final πN momentum, the spin-isospin matrix elements for each operator in Eq. (B.4) are evaluated. By using Eq. (B.3) and the corresponding resulting matrix elements of $T^\alpha_{\pi N,\gamma N}$, we can determine the invariant amplitudes J_i^α by solving a simple 2×2 matrix problem. The multipole amplitudes are then found by numerical integration via. Eq. (B.1).

We have checked our numerical procedure of calculating the multipole amplitudes by reproducing the Born term results provided by Wittman, and published by Laget.[8]

Since the E_{1+} to M_{1+} ratio of the $\Delta \to N\gamma$ transition is an important quantity, we explicitly show its definition and relations among authors. For the $\Delta \to N\gamma$ transition, there exist two sets of coupling schemes which are the analogs of the γNN Dirac and Sachs form factors, respectively. Both are, of course, equivalent for on-shell matrix elements. Ref. 6, for example, starts with the Dirac type coupling scheme (Eq. (1) of Ref. 6). Namely, the amplitude corresponding to Eqs. (2.9) is given as

$$M^\Delta = ie_0\overline{w}^\nu(p_\Delta,s_\Delta)\Gamma'_{\nu\mu}u_N(p_N,s_N)\epsilon^\mu(q,\lambda) \tag{B.5a}$$

with

$$\Gamma'_{\nu\mu} = \frac{g_1}{2m_N}(q_\nu\gamma_\mu - \not{q}g_{\nu\mu})i\gamma_5 - \frac{g_2}{(2m_N)^2}(q_\nu P_\mu - q\cdot P g_{\nu\mu})i\gamma_5, \tag{B.5b}$$

where $q = p_\Delta - p_N$ and $P = (p_\Delta + p_N)/2$. Isospin indices are dropped in Eqs. (B.5). In this coupling scheme, the M_{1+} and E_{1+} amplitudes of the $\Delta \to N\gamma$ transition are written as[6]

$$f_{M1} = \frac{e_0}{12m_N}\left(\frac{|\vec{q}\,|}{m_\Delta m_N}\right)^{1/2}\left[g_1(3m_\Delta + m_N) - g_2\frac{m_\Delta(m_\Delta - m_N)}{2m_N}\right] \tag{B.6a}$$

$$f_{E2} = -\frac{e_0}{6m_N}\frac{|\vec{q}\,|}{(m_\Delta + m_N)}\left(\frac{|\vec{q}\,|m_\Delta}{m_N}\right)^{1/2}\left[g_1 - g_2\frac{m_\Delta}{2m_N}\right] \tag{B.6b}$$

In the Δ-rest frame, the photon momentum is $|\vec{q}\,| = (m_\Delta^2 - m_N^2)/2m_\Delta$. Therefore the ratio R_{EM} is expressed as

$$R_{EM} = f_{E2}/f_{M1} = -\frac{m_\Delta - m_N}{2m_N}\frac{g_1 - g_2(\frac{m_\Delta}{2m_N})}{g_1\frac{(3m_\Delta+m_N)}{2m_N} - g_2\frac{m_\Delta(m_\Delta-m_N)}{(2m_N)^2}} \tag{B.6c}$$

By inserting the best values $g_1 = 4.8$ and $g_2 = 5.7$ of Ref. 6 into Eq. (B.6c) one obtains their quoted value $R_{EM} = -1.5\%$.

In the present paper we start with the alternative Sachs type form factors G_M and G_E of Eq. (2.10a). They are directly related to the magnetic dipole and electric quadrapole transitions. At $q^2 = 0$, G_M and G_E are related to g_1 and g_2 by[25]

$$\frac{g_1}{2m_N} = \frac{3}{2}\frac{1}{m_\Delta + m_N}\frac{m_\Delta}{m_N}(G_M - G_E) \tag{B.7a}$$

$$\frac{g_2}{(2m_N)^2} = \frac{3}{2}\frac{1}{m_N(m_\Delta + m_N)}(G_M - G_E\frac{3m_\Delta + m_N}{m_\Delta - m_N}) \tag{B.7b}$$

By inserting Eqs. (B.7) into Eqs. (B.6), the amplitudes and the ratio in this coupling scheme are written as

$$f_{M1} = \frac{e_0}{2m_N}\left(\frac{|\vec{q}\,|m_\Delta}{m_N}\right)^{1/2}G_M \tag{B.8a}$$

$$f_{E2} = -\frac{e_0}{2m_N}\left(\frac{|\vec{q}\,|m_\Delta}{m_N}\right)^{1/2}\frac{2|\vec{q}\,|m_\Delta}{m_\Delta^2 - m_N^2}G_E \tag{B.8b}$$

$$R_{EM} = f_{E2}/f_{M1} = -G_E/G_M. \tag{B.8c}$$

The present values of $G_M = 2.28$ and $G_E = 0.07$ give the ratio $R_{EM} = -3.1\%$. Using Eqs. (B.7), $G_M = 2.28$ and $G_E = 0.07$ are transformed into $g_1 = 3.8$ and $g_2 = 3.0$. These numbers are to be compared with $g_1 = 4.8$ and $g_2 = 5.7$ of Ref. 6.

C. Conventions for amplitudes and observables

i) Scattering amplitudes

In the present paper we use the relativistic conventions of Bjorken and Drell,[26] as well as the non-relativistic conventions of Goldberger and Watson.[30] In particular, our invariant scattering amplitude M, is related to the S-matrix by

$$S = 1 - i(2\pi)^4\delta^4(P_f - P_i)\frac{M}{N} \tag{C.1}$$

where N is a product of factors, one for each particle i of energy E_i and mass m_i

$$N = \prod_i \begin{cases} (2\pi)^{3/2}(2E_i)^{1/2} & \text{for bosons} \\ (2\pi)^{3/2}(E_i/m_i)^{1/2} & \text{for fermions.} \end{cases} \qquad (C.2)$$

Similarly our non-relativistic t-matrix T obeys the relation

$$S = 1 - i2\pi\delta^4(P_f - P_i)T. \qquad (C.3)$$

For the case of pion photoproduction, the two scattering amplitudes are therefore related by

$$T_{\pi N,\gamma N}(\vec{k}\vec{p}', \vec{q}\vec{p}) = (2\pi)^3 F_\pi(\vec{k})F_N(\vec{p}')F_\gamma(\vec{q})F_N(\vec{p})M_{\pi N,\gamma N}(\vec{k}\vec{p}', \vec{q}\vec{p}) \qquad (C.4)$$

where

$$F_\pi(\vec{k}) = \frac{1}{(2\pi)^{3/2}}\frac{1}{\sqrt{2E_\pi(\vec{k})}}, \qquad (C.5a)$$

$$F_\gamma(\vec{q}) = \frac{1}{(2\pi)^{3/2}}\frac{1}{\sqrt{2E_\gamma(\vec{q})}}, \qquad (C.5b)$$

$$F_N(\vec{p}) = \frac{1}{(2\pi)^{3/2}}\sqrt{\frac{m_N}{E_N(\vec{p})}}. \qquad (C.5c)$$

It is often useful to reexpress Eq. (C.3) in terms of partial wave amplitudes. For πN scattering, for example, the on-shell t-matrix in a given eigenchannel of total angular momentum j, total isospin t and orbital angular momentum ℓ, is related to the s-matrix by

$$S^{\ell jt}_{\pi N,\pi N}(k,k,E) = e^{2i\delta^{jt}_\ell} = 1 - 2\pi i\rho(k)T^{\ell jt}_{\pi N,\pi N}(k,k,E) \qquad (C.6)$$

where δ^{jt}_ℓ is the phase shift and the density of states is

$$\rho(k) = \frac{E_N(k)E_\pi(k)k}{E_N(k) + E_\pi(k)}. \qquad (C.7)$$

ii) Differential cross section

The differential cross section for pion photoproduction, in the center of mass frame, is given by

$$\frac{d\sigma}{d\Omega_{CM}} = \frac{1}{16\pi^2}\frac{k}{\omega_q}\frac{m_N^2}{E^2}\frac{1}{4}\sum_{s',s,\lambda} |< \vec{k}, s'|M_{\pi N,\gamma N}(E)|\vec{q}, \lambda, s >|^2 \qquad (C.8)$$

where $\omega_q = |\vec{q}|$ and λ are the energy and polarization of the photon, respectively. The total energy is $E=E_p+\omega_q$, where $\vec{p} = -\vec{q}$. The pion momentum $k=|\vec{k}|$ is given by energy conservation as

$$k = \frac{1}{2E}\sqrt{(E^2 + m_\pi^2 - m_N^2)^2 - 4m_\pi^2E^2}. \qquad (C.9)$$

iii) γ-asymmetry

The γ-asymmetry is defined by

$$\Sigma = \frac{\sigma_\perp - \sigma_\parallel}{\sigma_\perp + \sigma_\parallel}, \qquad (C.10)$$

where $\sigma_\perp$ ($\sigma_\parallel$) is the differential cross section Eq. (C.8) for the photon polarization normal (parallel) to the production plane defined by the vector $(\vec{q}\times\vec{k})$, where $\vec{q}$ is the incident photon momentum and $\vec{k}$ is the outgoing pion momentum. We follow the usual convention of choosing the photon direction along the z-axis and defining the xz-plane as the scattering plane. Thus the vector $(\vec{q}\times\vec{k})$ is along the y-axis. In this convention, we can choose the photon polarization vectors as follows: $\epsilon^\mu_\perp \equiv \epsilon^\mu(q,\lambda=+1)$=(0,1,0,0) for $\sigma_\perp$ and $\epsilon^\mu_\parallel \equiv \epsilon^\mu(q,\lambda=-1)$=(0,0,1,0) for $\sigma_\parallel$, respectively.

iv) Target asymmetry

The Target asymmetry is defined by

$$T = \frac{\sigma^t_\uparrow - \sigma^t_\downarrow}{\sigma^t_\uparrow + \sigma^t_\downarrow}, \qquad (C.11)$$

where $\sigma^t_\uparrow(\sigma^t_\downarrow)$ is the differential cross section Eq. (C.8) for the target nucleon spin polarization parallel (anti-parallel) to the vector $(\vec{q}\times\vec{k})$. Therefore the target nucleon spinors χ_s ($s=\pm1/2$) are chosen to be eigenstates of σ_y instead of σ_z. Namely $\chi_{\pm1/2} = 1/\sqrt{2}(1, \pm i)$, where $s=+1/2$ and $s=-1/2$ correspond to the cases of $\sigma^t_\uparrow$ and $\sigma^t_\downarrow$, respectively.

v) Recoil nucleon asymmetry

The recoil nucleon asymmetry is defined by

$$P = \frac{\sigma^r_\uparrow - \sigma^r_\downarrow}{\sigma^r_\uparrow + \sigma^r_\downarrow}, \qquad (C.12)$$

where $\sigma^r_\uparrow(\sigma^r_\downarrow)$ is the differential cross section Eq. (C.8) for the recoil nucleon spin polarization parallel (anti-parallel) to the vector $(\vec{q}\times\vec{k})$. Therefore the recoil nucleon spinors $\chi_{s'}$ ($s'=\pm1/2$) are chosen to be eigenstates of σ_y. Namely $\chi_{\pm1/2} = 1/\sqrt{2}(1, \pm i)$, where $s'=+1/2$ and $s'=-1/2$ correspond to the cases of $\sigma^r_\uparrow$ and $\sigma^r_\downarrow$, respectively.

Table 1: Coupling constants of the mesonic and electromagnetic vertices of the Lagrangian given in Section II.

e_0	$\sqrt{1/137 \cdot 4\pi}$	
$f_{\pi NN}$	$\sqrt{0.08 \cdot 4\pi}$	Eqs. (2.2)
κ_p	+1.79	
κ_n	−1.91	
$g_{\rho NN}$	2.66	
K_V	6.6	
$g_{\rho\pi\gamma}$	$0.374e_0/3$	
		Eqs. (2.3)
$g_{\omega NN}$	$2.66 \cdot 3$	
K_S	0.0	
$g_{\omega\pi\gamma}$	$0.374e_0$	
$G_M(0)$	see the text	
		Eq. (2.10a)
$G_E(0)$	see the text	

Table 2: Parameters of the form factors, Eqs. (A.4) and (A.11), for the πN separable potential $V_{\pi N,\pi N}$. a_1 is in units of $[fm]^{-2n_1+m_1+\ell+1}$. a_2 is in units of $[fm]^{-2n_2+m_2+\ell+1/2}$ for P_{11} and P_{33} partial waves, otherwise is in units of $[fm]^{-2n_2+m_2+\ell+1}$.

$L_{2t,2j}$	ℓ	m_1	n_1	a_1	$b_1(fm^{-1})$	m_2	n_2	a_2	$b_2(fm^{-1})$	λ_0 or $\lambda_1(=\lambda_2)$
S_{11}	0	0	1	0.6622	1.447	2	2	7.037	3.648	−1
S_{31}	0	0	2	11.308	2.484	2	3	21.652	1.907	+1
P_{11}	1	2	3	31.623	2.665	0	2	0.5793	1.185	−1
P_{13}	1	0	2	0.4269	1.181	2	3	3.970	1.721	+1
P_{31}	1	0	2	1.473	1.542	2	3	8.053	1.861	+1
P_{33}	1	0	2	2.770	1.415	0	2	1.778	1.218	+1
D_{13}	2	0	2	1.639	2.615	2	3	9.312	3.263	−1
D_{15}	2	0	2	0.2172	1.175	2	3	1.011	1.461	−1
D_{33}	2	0	2	0.1306	1.128	2	3	1.081	1.972	−1
D_{35}	2	0	2	0.2270	1.168	2	3	1.151	1.780	+1

Table 3: Cloudy bag model P_{33} potential parameters. Eq. (3.14) and Eq. (A.4a) are used for the pole term and the background term, respectively.

$R(fm)$	$f_{\pi N\Delta}$	m_1	n_1	$a_1(fm^2)$	$b_1(fm^{-1})$	λ_0
0.8	2.836	4	2	0.277	2.181	−1
1.0	3.50	4	2	0.234	2.649	−1
1.2	3.50	4	2	0.235	2.405	−1

Figure Captions

Fig. 1 The basic mechanisms for pion photoproduction considered in this work: Born terms (a) $\sim$ (f) and Δ excitation term (g).

Fig. 2 Fits to the πN phase shifts of Ref. 37 for each partial wave $L_{2I,2J}$ using the separable potentials of Eqs. (A.3) and (A.10). The corresponding πN parameters are listed in Table 2. The P_{33} results calculated using the parameters of Table 3 are indistinguishable and therefore not shown. The resulting off-shell t-matrix $T_{\pi N,\pi N}$ provides the final state interaction in our calculation.

Fig. 3 The calculated $M_{1+}(3/2)$ and $E_{1+}(3/2)$ multipole amplitudes compared with the data.[33,34] Solid curves are from the full unitary calculation. Dashed curves are the contributions from the non-resonant terms only. These calculations correspond to the model parameters G_M=2.28, G_E=0.07 and Λ=650 MeV/c.

Fig. 4 Calculated differential cross sections of $\gamma n \to \pi^- p$ reaction compared with the data.[32] The model parameters are the same as in Fig. 3.

Fig. 5 Same as Fig. 4, but for $\gamma p \to \pi^+ n$ reaction.

Fig. 6 Same as Fig. 4, but for $\gamma p \to \pi^0 p$ reaction.

Fig. 7 Calculated differential cross sections of $\gamma n \to \pi^- p$ compared with the TRIUMF data.[35] The model parameters are the same as in Fig. 3.

Fig. 8 Calculated total cross sections of (a) $\gamma n \to \pi^- p$, (b) $\gamma p \to \pi^+ n$, and (c) $\gamma p \to \pi^0 p$ reactions compared with the data.[32,35] The model parameters are the same as in Fig. 3.

Fig. 9 The differential cross sections calculated with cut-off parameter Λ = 350 MeV/c (short-dashed curves), 650 MeV/c (solid curves) and 900 MeV/c (long-dashed curves). Data are taken from Ref. 32.

Fig. 10 The solid curves are $M_{1+}(3/2)$ and $E_{1+}(3/2)$ multipole amplitudes calculated from a non-unitary model neglecting the effect of πN final state interactions on the *Born* terms. The dashed curves are the contributions from the Born terms only. Data are from Refs. 33 and 34.

Fig. 11 The differential cross sections from the full unitary calculation (solid curves), and the on-shell approximation where we set the (PV) term of Eq.(4.10) to zero, and $\Lambda = \infty$ (dashed curves). Data are from Ref. 32.

Fig. 12 Same as Fig. 11, but for the calculations of the $M_{1+}(3/2)$ and $E_{1+}(3/2)$ multipole amplitudes. Data are from Refs. 33 and 34.

Fig. 13 The best fits to the $M_{1+}(3/2)$ and $E_{1+}(3/2)$ multipole amplitudes in the calculations using the on-shell approximation with $\Lambda = \infty$. Data points are taken from Refs. 33 and 34.

Fig. 14 Sensitivity of the differential cross sections to the vector meson exchange diagrams of Figs. 1(e) and 1(g). Solid curves are with meson exchange, dashed curves are without. Data are from Ref. 32.

Fig. 15 Same as Fig. 14, but for multipole amplitudes. Data points are taken from Refs. 33 and 34.

Fig. 16 Calculated γ-asymmetries compared with the data.[32]

Fig. 17 Calculated Target asymmetries compared with the data.[32]

Fig. 18 Calculated Recoil nucleon asymmetries compared with the data.[32]

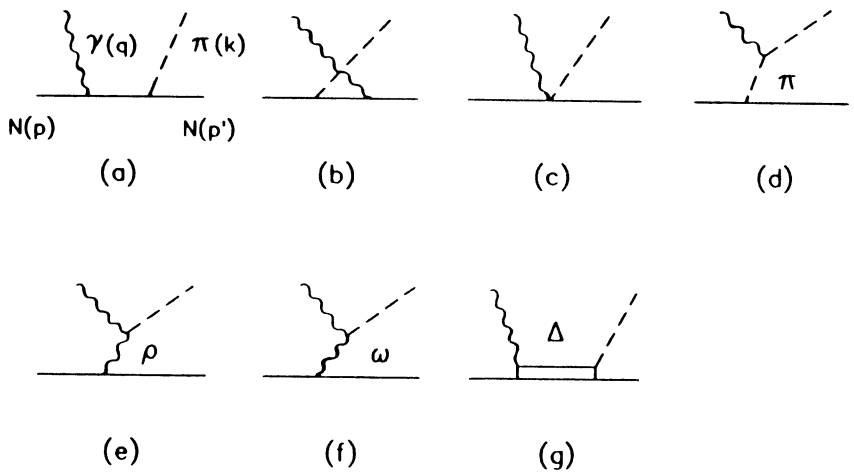
γ(q)
π(k)
N(p)
N(p')
(a)
(b)
(c)
π
(d)
ρ
(e)
ω
(f)
Δ
(g)

Fig. 1

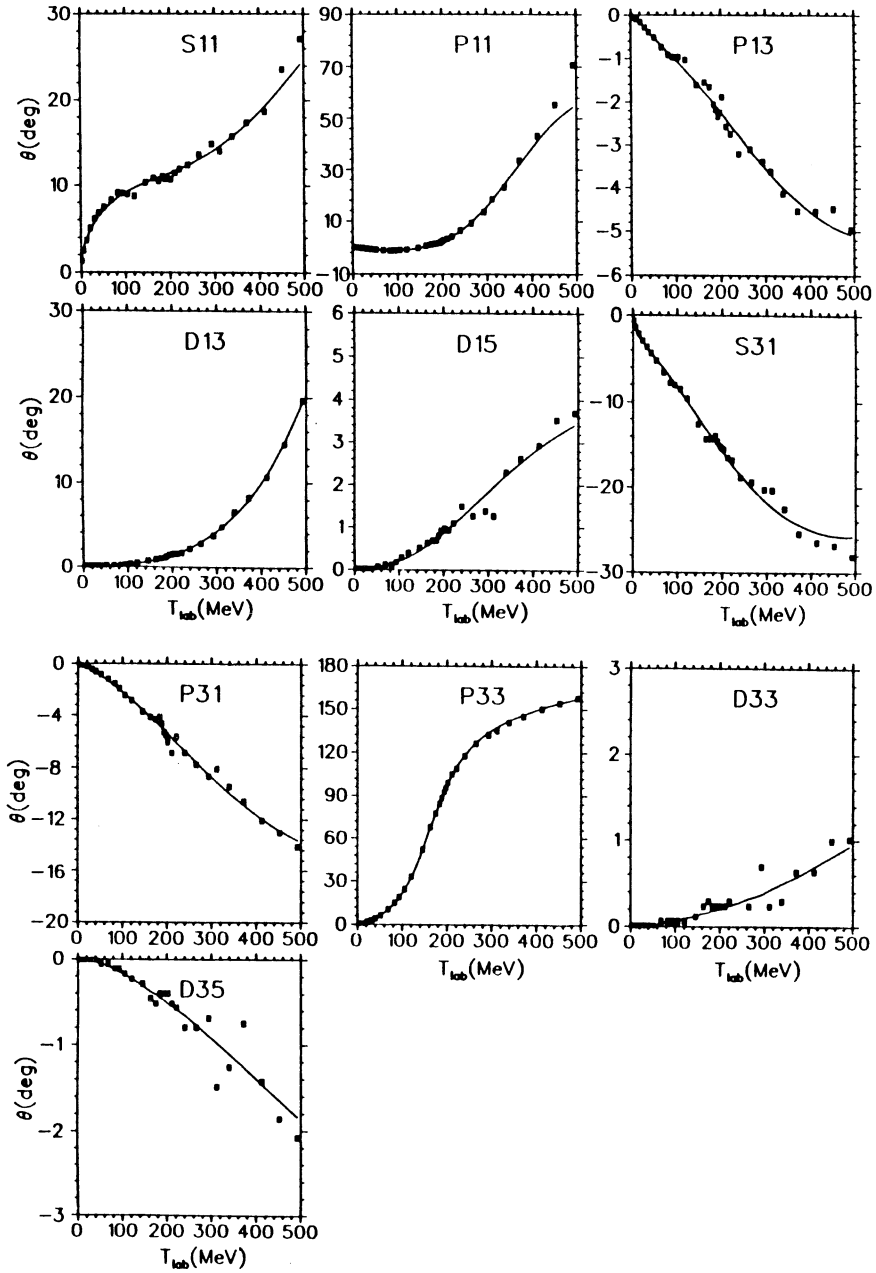
S11
P11
P13
D13
D15
S31
P31
P33
D33
D35
θ(deg)
T_lab(MeV)

Fig. 2

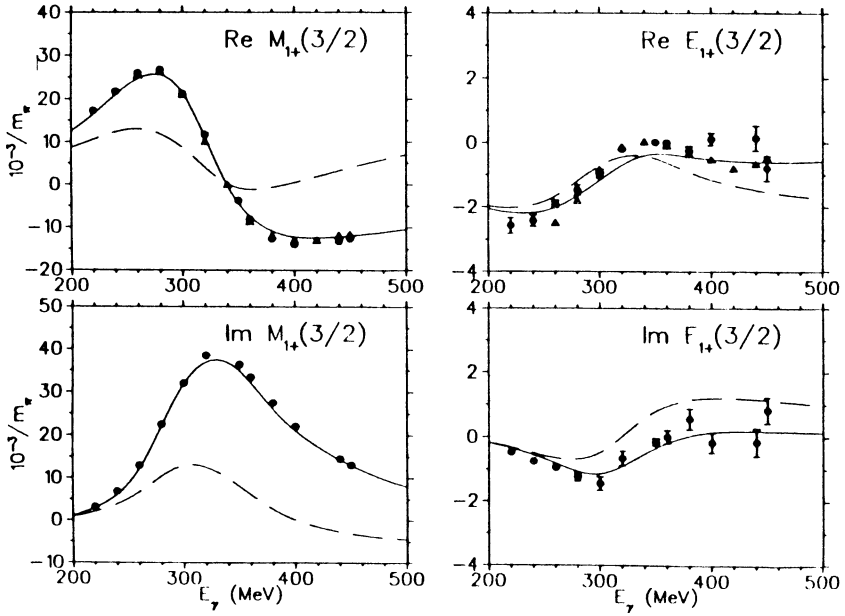
Re $M_{1+}(3/2)$
Re $E_{1+}(3/2)$
Im $M_{1+}(3/2)$
Im $E_{1+}(3/2)$
$10^{-3}/m_\pi$
E_γ (MeV)

Fig. 3

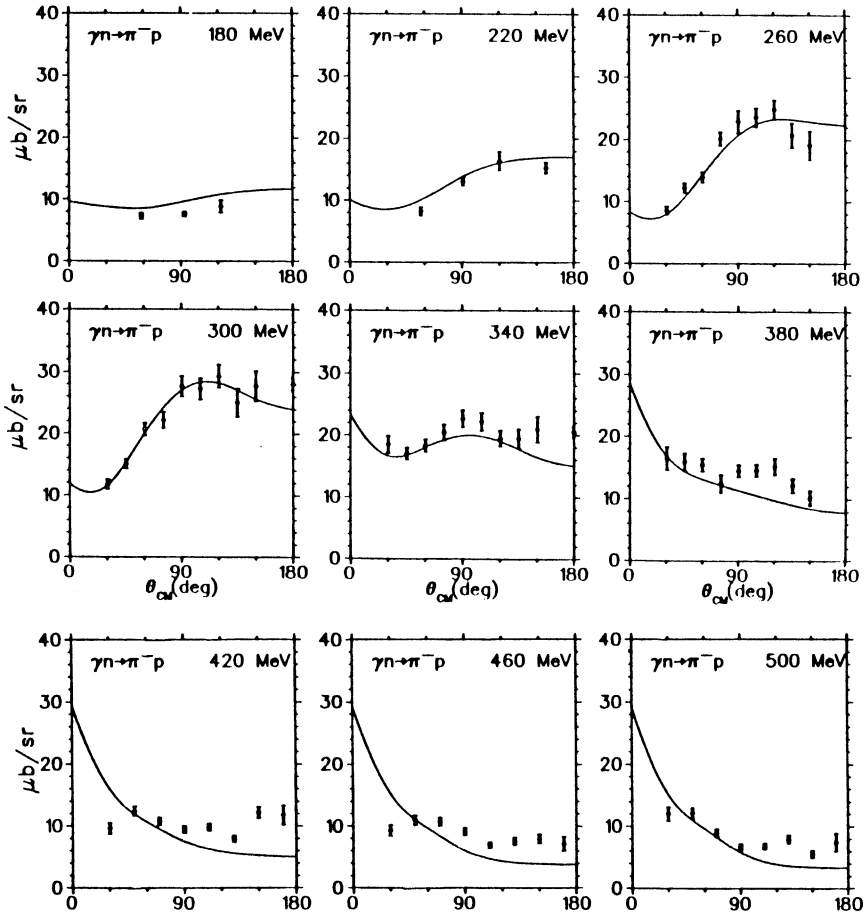
$\gamma n \to \pi^- p$ 180 MeV
$\gamma n \to \pi^- p$ 220 MeV
$\gamma n \to \pi^- p$ 260 MeV
$\gamma n \to \pi^- p$ 300 MeV
$\gamma n \to \pi^- p$ 340 MeV
$\gamma n \to \pi^- p$ 380 MeV
$\gamma n \to \pi^- p$ 420 MeV
$\gamma n \to \pi^- p$ 460 MeV
$\gamma n \to \pi^- p$ 500 MeV
$\mu b/sr$
θ_{CM} (deg)

Fig. 4

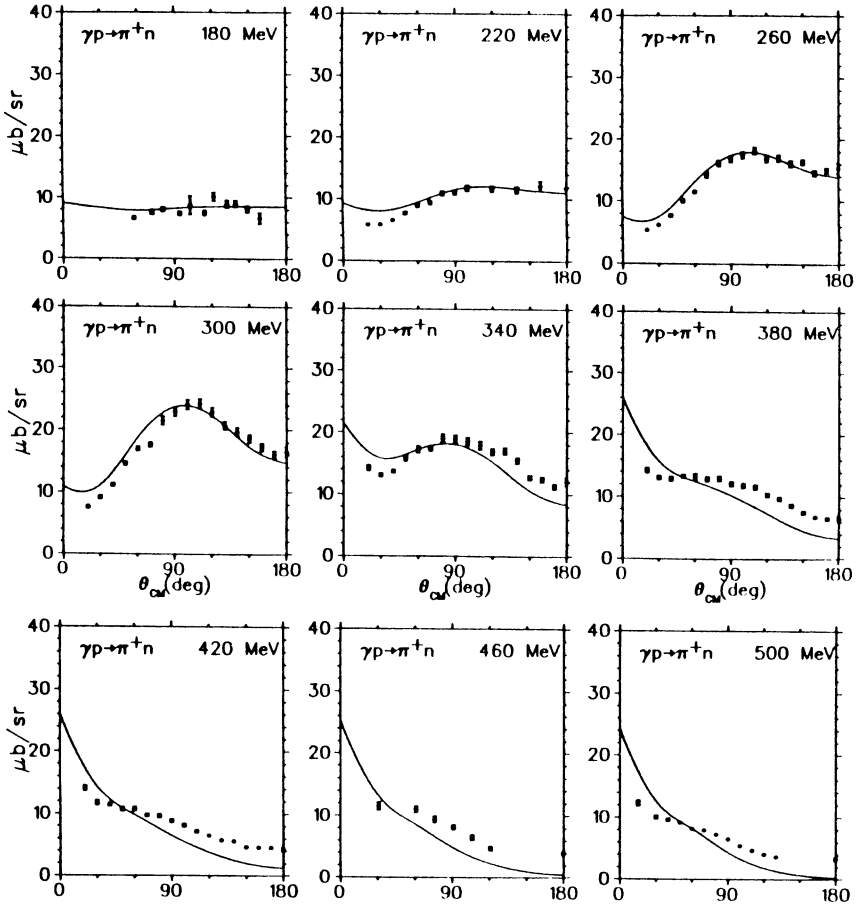
γp→π+n 180 MeV
γp→π+n 220 MeV
γp→π+n 260 MeV
γp→π+n 300 MeV
γp→π+n 340 MeV
γp→π+n 380 MeV
γp→π+n 420 MeV
γp→π+n 460 MeV
γp→π+n 500 MeV
μb/sr
θCM(deg)

Fig. 5

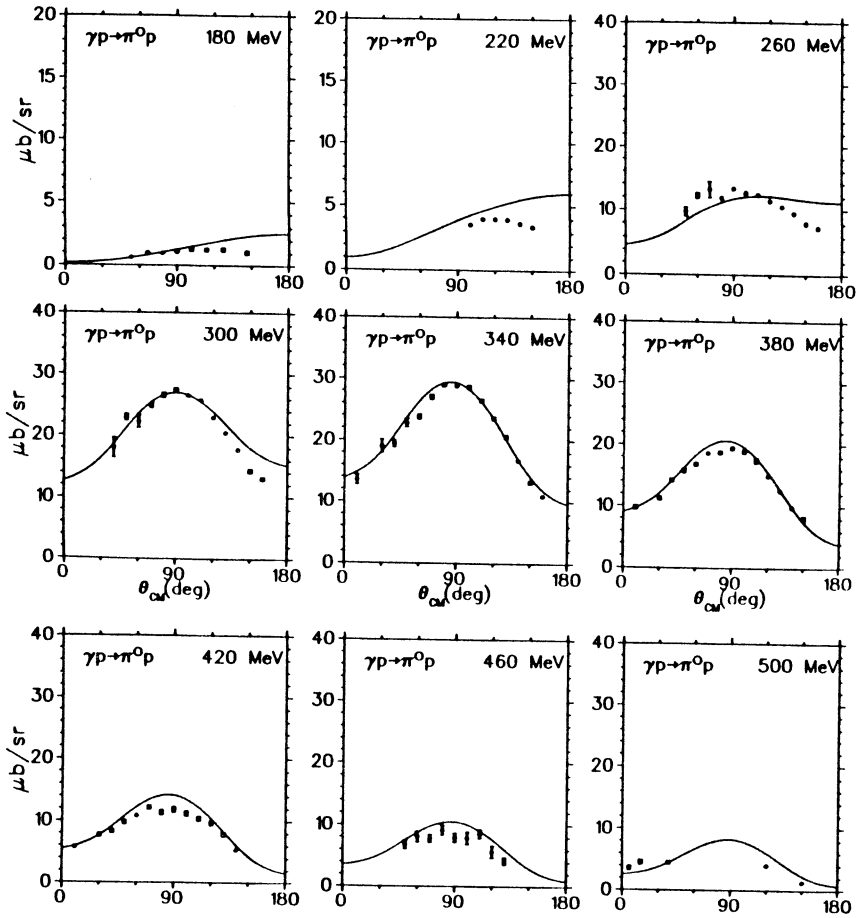
γp→π°p 180 MeV
γp→π°p 220 MeV
γp→π°p 260 MeV
γp→π°p 300 MeV
γp→π°p 340 MeV
γp→π°p 380 MeV
γp→π°p 420 MeV
γp→π°p 460 MeV
γp→π°p 500 MeV
μb/sr
θCM(deg)

Fig. 6

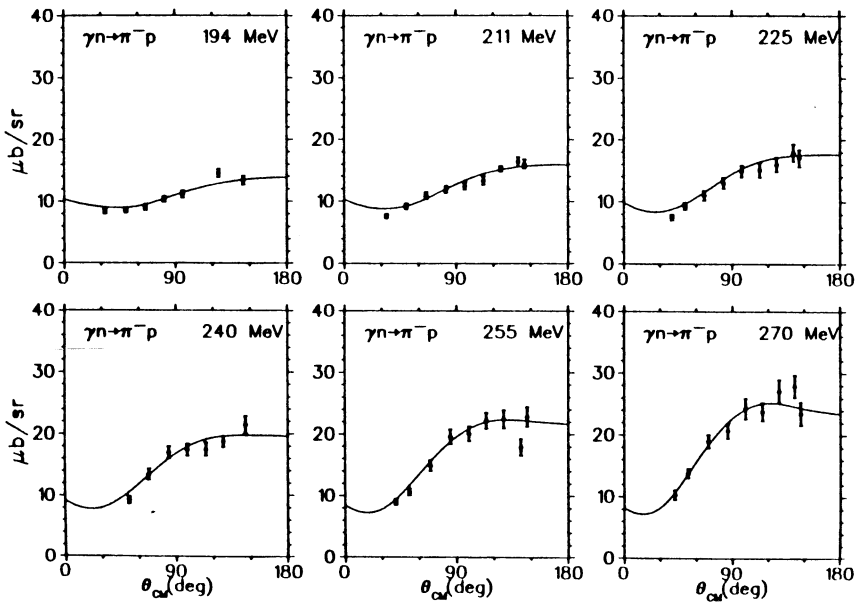
γn→π⁻p 194 MeV
γn→π⁻p 211 MeV
γn→π⁻p 225 MeV
γn→π⁻p 240 MeV
γn→π⁻p 255 MeV
γn→π⁻p 270 MeV
μb/sr
θ_CM(deg)

Fig. 7

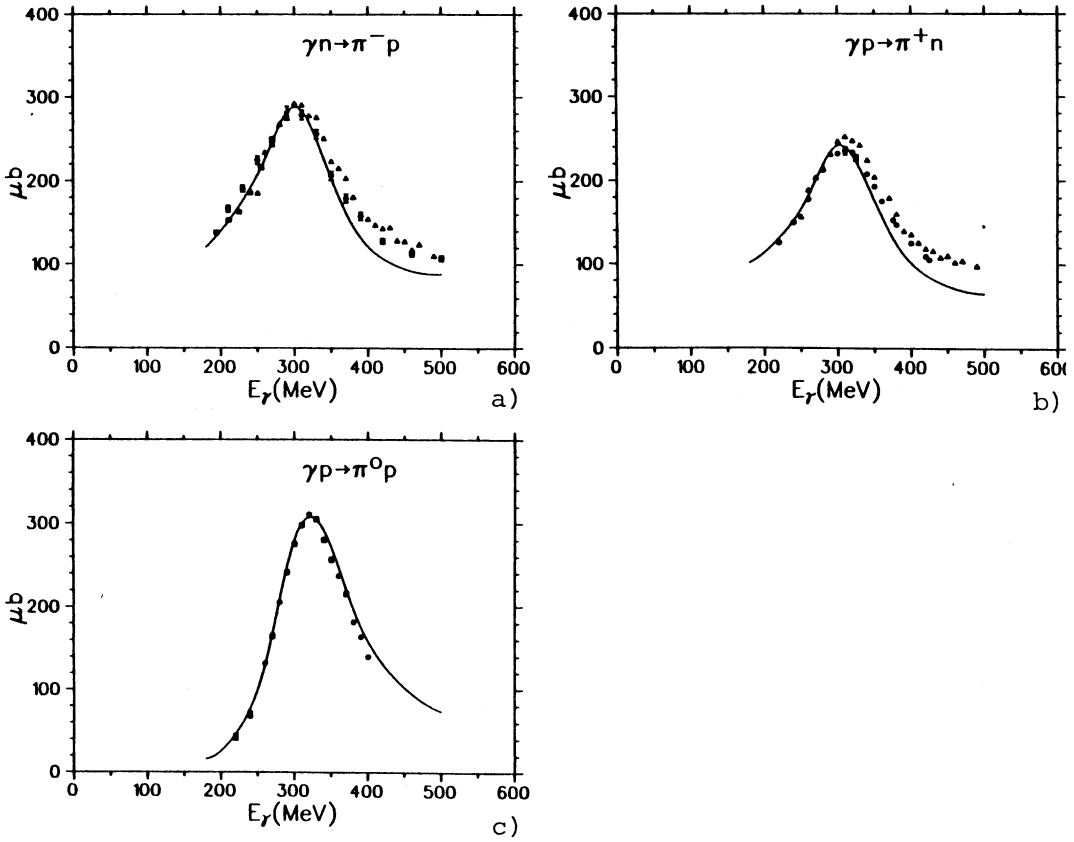
γn→π⁻p
γp→π⁺n
γp→π⁰p
μb
E_γ(MeV)
a)
b)
c)

Fig. 8

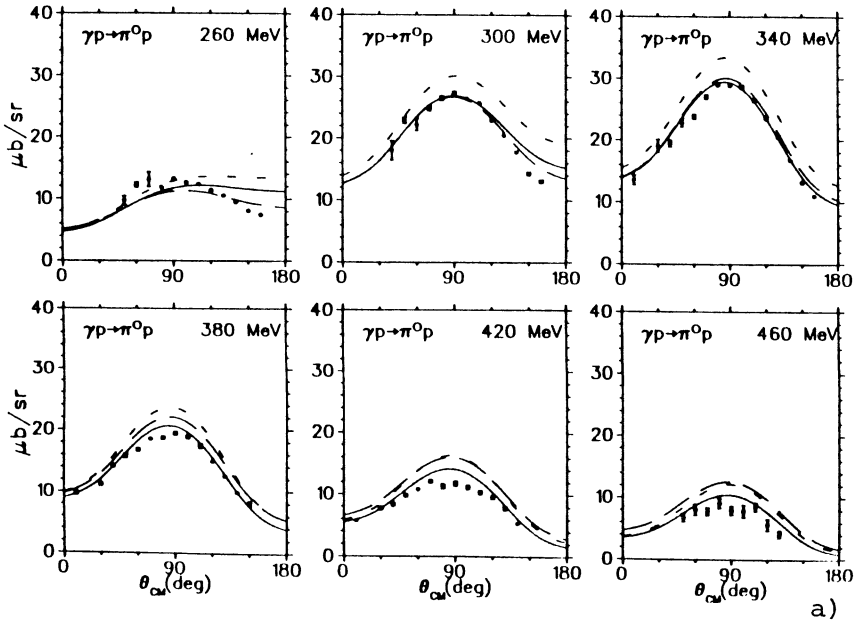
γp→π⁰p 260 MeV
γp→π⁰p 300 MeV
γp→π⁰p 340 MeV
γp→π⁰p 380 MeV
γp→π⁰p 420 MeV
γp→π⁰p 460 MeV
μb/sr
θ_CM (deg)
a)

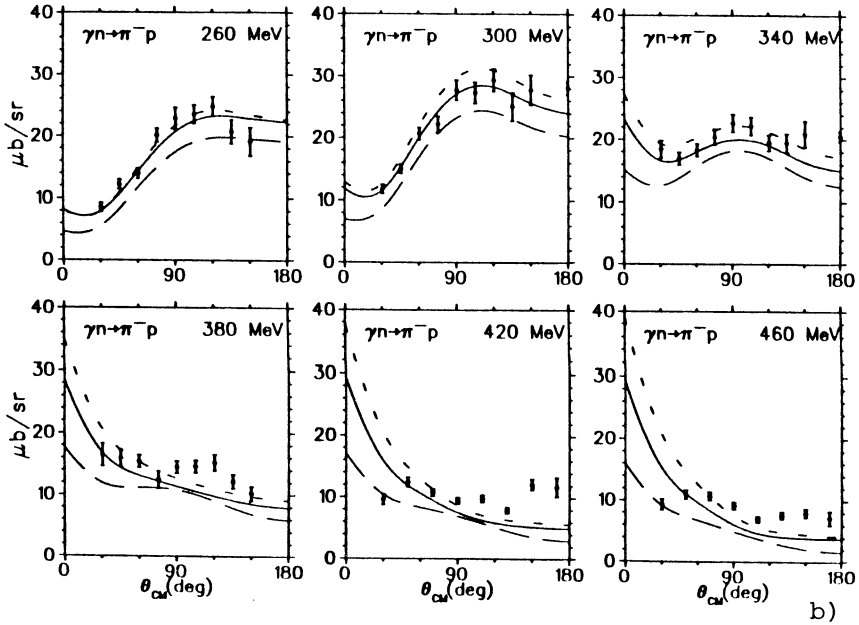
γn→π⁻p 260 MeV
γn→π⁻p 300 MeV
γn→π⁻p 340 MeV
γn→π⁻p 380 MeV
γn→π⁻p 420 MeV
γn→π⁻p 460 MeV
μb/sr
θ_CM (deg)
b)

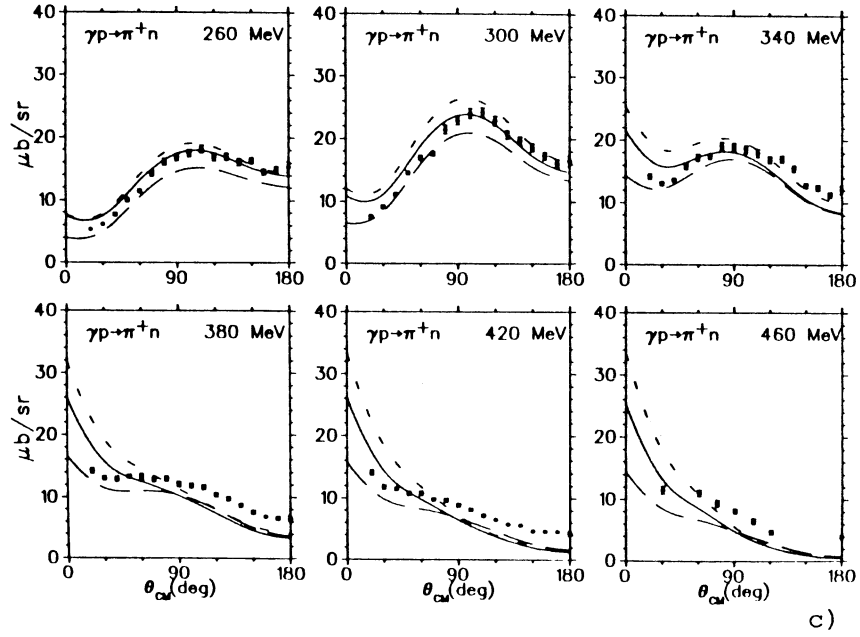
γp→π⁺n 260 MeV
γp→π⁺n 300 MeV
γp→π⁺n 340 MeV
γp→π⁺n 380 MeV
γp→π⁺n 420 MeV
γp→π⁺n 460 MeV
μb/sr
θ_CM (deg)
c)

Fig. 9

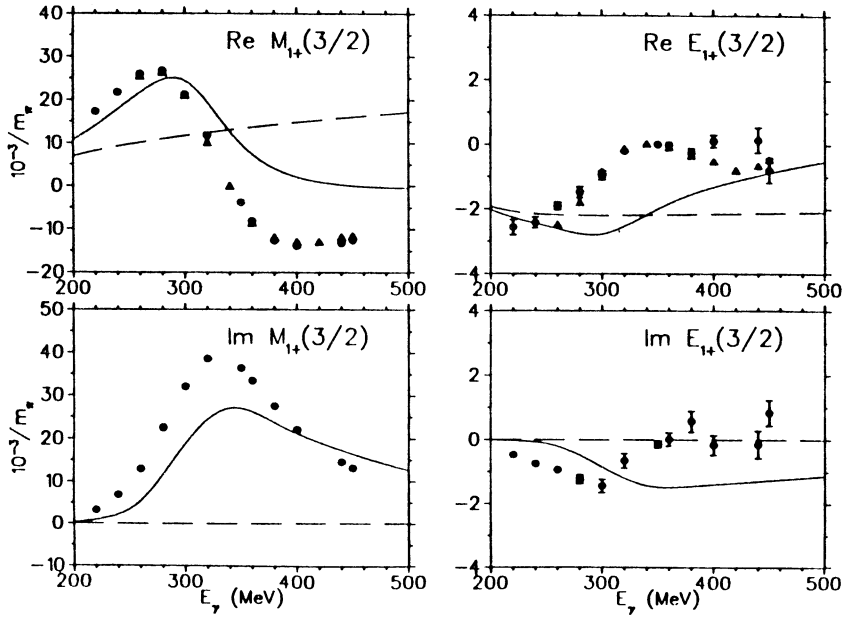
Re M1+(3/2)
Re E1+(3/2)
Im M1+(3/2)
Im E1+(3/2)
10⁻³/Eπ
Eγ (MeV)

Fig. 10

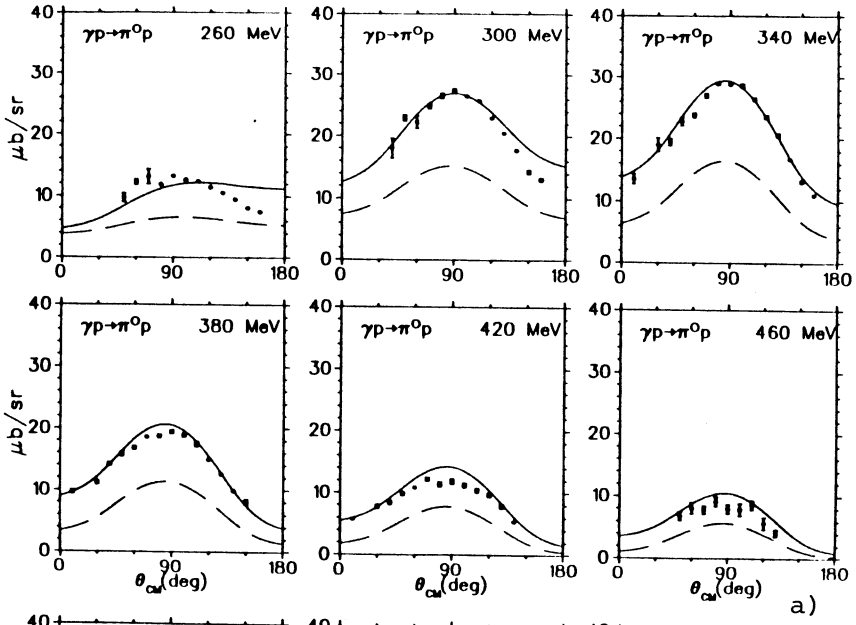
γp→π°p 260 MeV
γp→π°p 300 MeV
γp→π°p 340 MeV
γp→π°p 380 MeV
γp→π°p 420 MeV
γp→π°p 460 MeV
μb/sr
θ_CM (deg)
a)

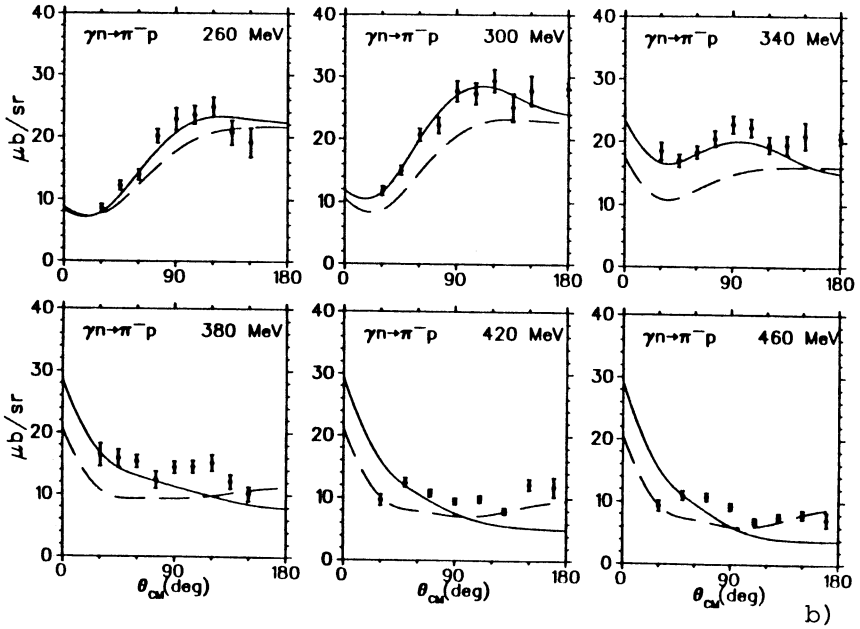
γn→π⁻p 260 MeV
γn→π⁻p 300 MeV
γn→π⁻p 340 MeV
γn→π⁻p 380 MeV
γn→π⁻p 420 MeV
γn→π⁻p 460 MeV
μb/sr
θ_CM (deg)
b)

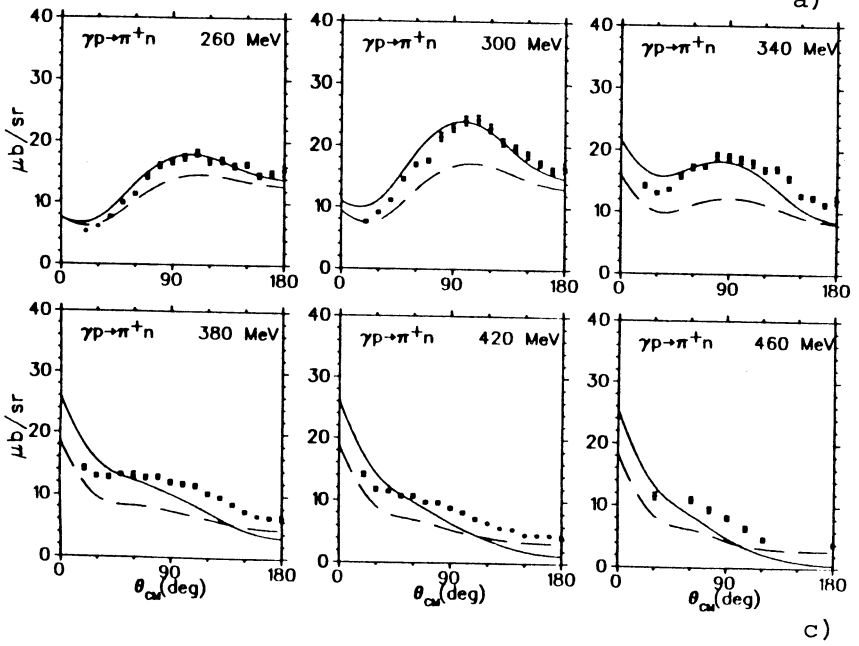
γp→π⁺n 260 MeV
γp→π⁺n 300 MeV
γp→π⁺n 340 MeV
γp→π⁺n 380 MeV
γp→π⁺n 420 MeV
γp→π⁺n 460 MeV
μb/sr
θ_CM (deg)
c)

Fig. 11

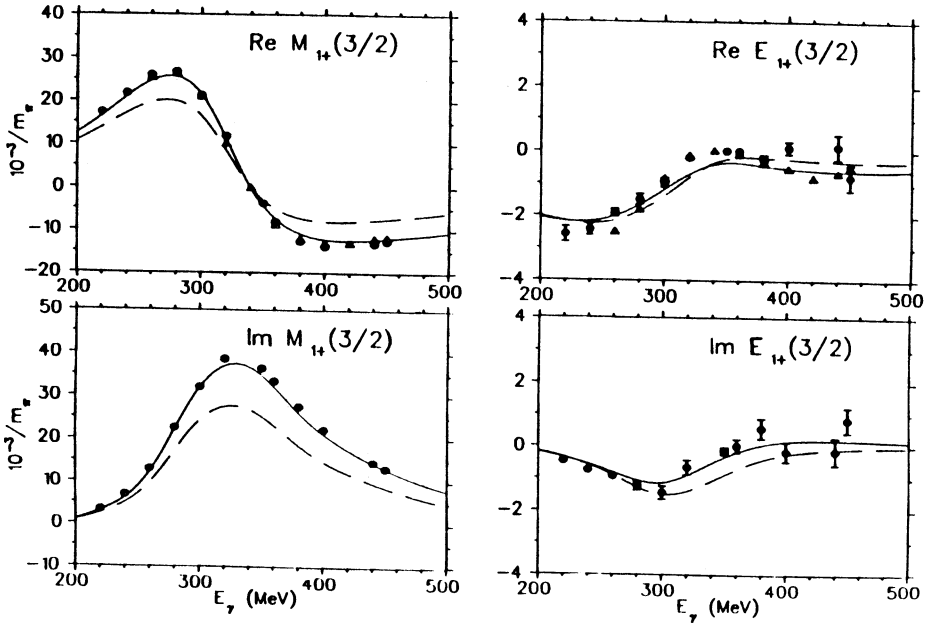
Re M 1+(3/2)
Im M 1+(3/2)
Re E 1+(3/2)
Im E 1+(3/2)
10⁻³/mπ
E_γ (MeV)

Fig. 12

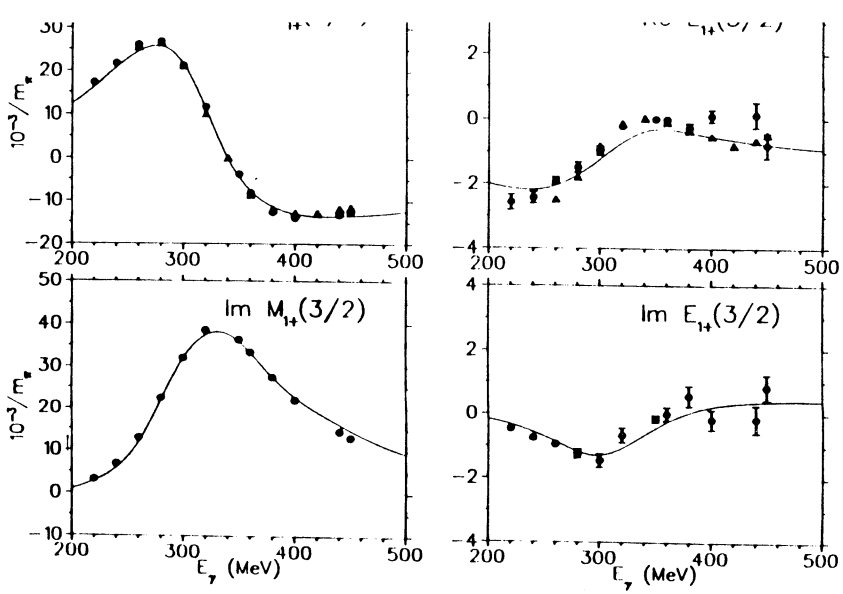
Im $M_{1+}(3/2)$
Im $E_{1+}(3/2)$
$10^{-3}/m_\pi$
E_γ (MeV)

Fig. 13

$\gamma p \to \pi^0 p$ 260 MeV
$\gamma p \to \pi^0 p$ 300 MeV
$\gamma p \to \pi^0 p$ 340 MeV
$\gamma p \to \pi^0 p$ 380 MeV
$\gamma p \to \pi^0 p$ 420 MeV
$\gamma p \to \pi^0 p$ 460 MeV
$\gamma n \to \pi^- p$ 260 MeV
$\gamma n \to \pi^- p$ 300 MeV
$\gamma n \to \pi^- p$ 340 MeV
$\gamma n \to \pi^- p$ 380 MeV
$\gamma n \to \pi^- p$ 420 MeV
$\gamma n \to \pi^- p$ 460 MeV
$\gamma p \to \pi^+ n$ 260 MeV
$\gamma p \to \pi^+ n$ 300 MeV
$\gamma p \to \pi^+ n$ 340 MeV
$\gamma p \to \pi^+ n$ 380 MeV
$\gamma p \to \pi^+ n$ 420 MeV
$\gamma p \to \pi^+ n$ 460 MeV
$\mu b/sr$
θ_{CM} (deg)
a)
b)
c)

Fig. 14

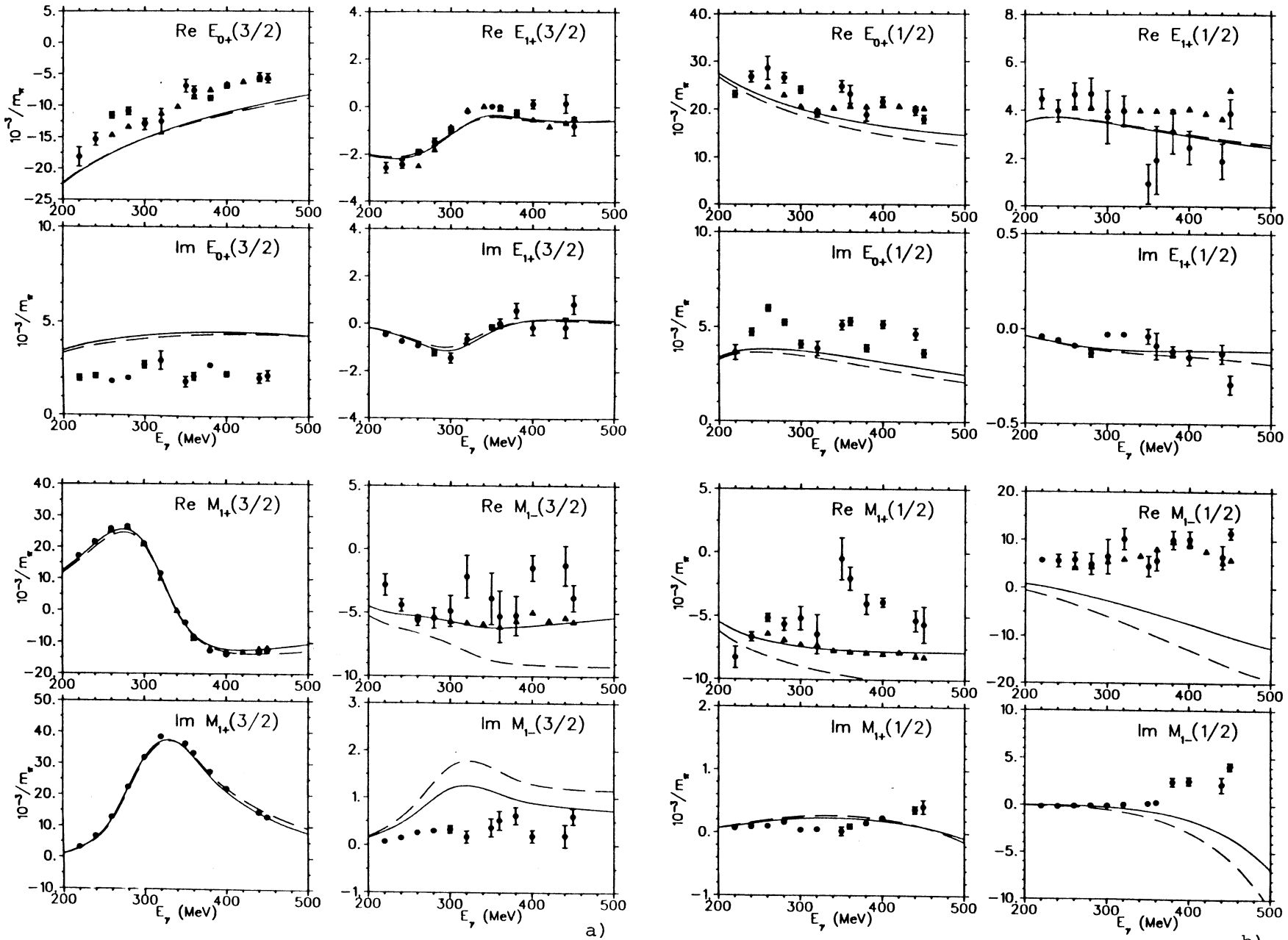
Re $E_{0+}(3/2)$
Re $E_{1+}(3/2)$
Re $E_{0+}(1/2)$
Re $E_{1+}(1/2)$
Im $E_{0+}(3/2)$
Im $E_{1+}(3/2)$
Im $E_{0+}(1/2)$
Im $E_{1+}(1/2)$
Re $M_{1+}(3/2)$
Re $M_{1-}(3/2)$
Re $M_{1+}(1/2)$
Re $M_{1-}(1/2)$
Im $M_{1+}(3/2)$
Im $M_{1-}(3/2)$
Im $M_{1+}(1/2)$
Im $M_{1-}(1/2)$
$10^{-3}/E_\pi$
E_γ (MeV)
a)
b)

Fig. 15

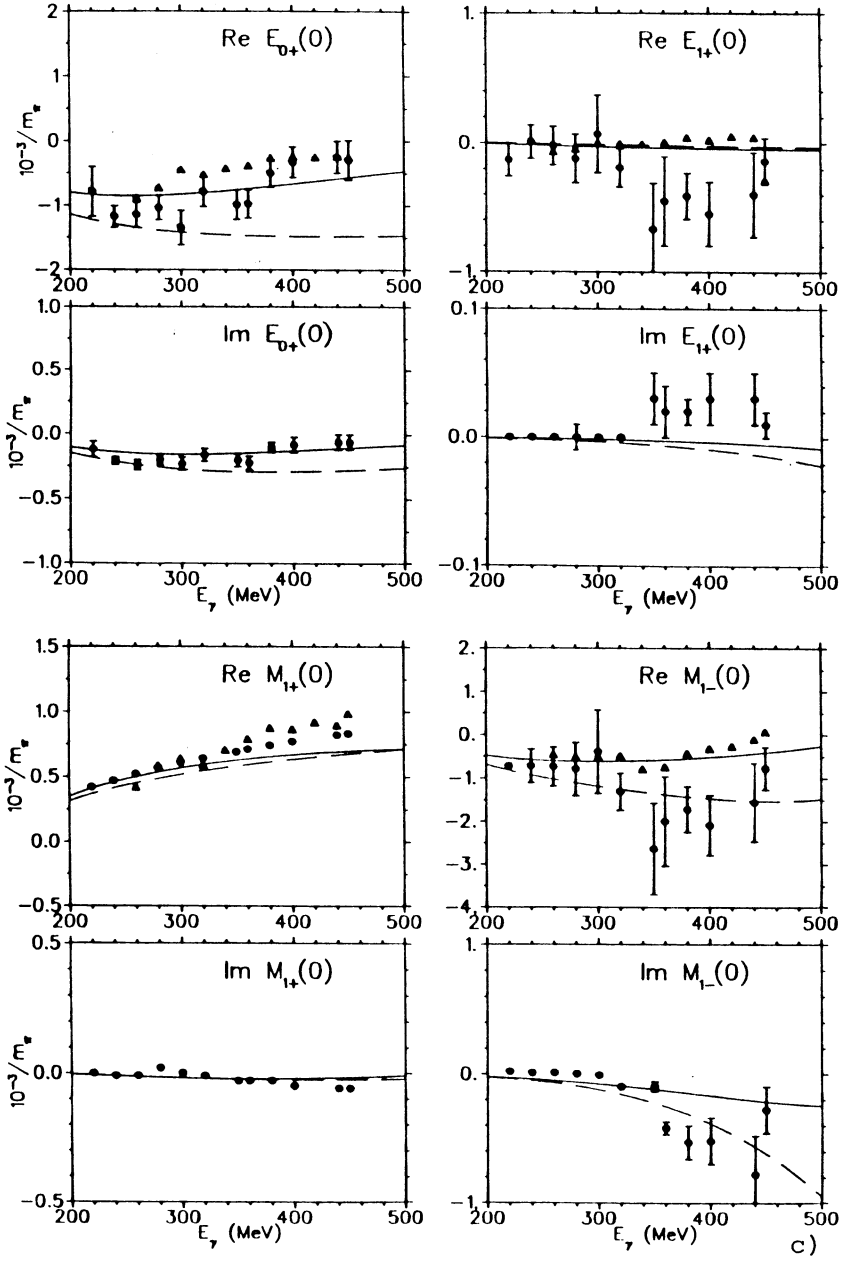
Re $E_{0+}(0)$
Re $E_{1+}(0)$
Im $E_{0+}(0)$
Im $E_{1+}(0)$
Re $M_{1+}(0)$
Re $M_{1-}(0)$
Im $M_{1+}(0)$
Im $M_{1-}(0)$
$10^{-3}/E_\pi$
E_γ (MeV)
c)

Fig. 15

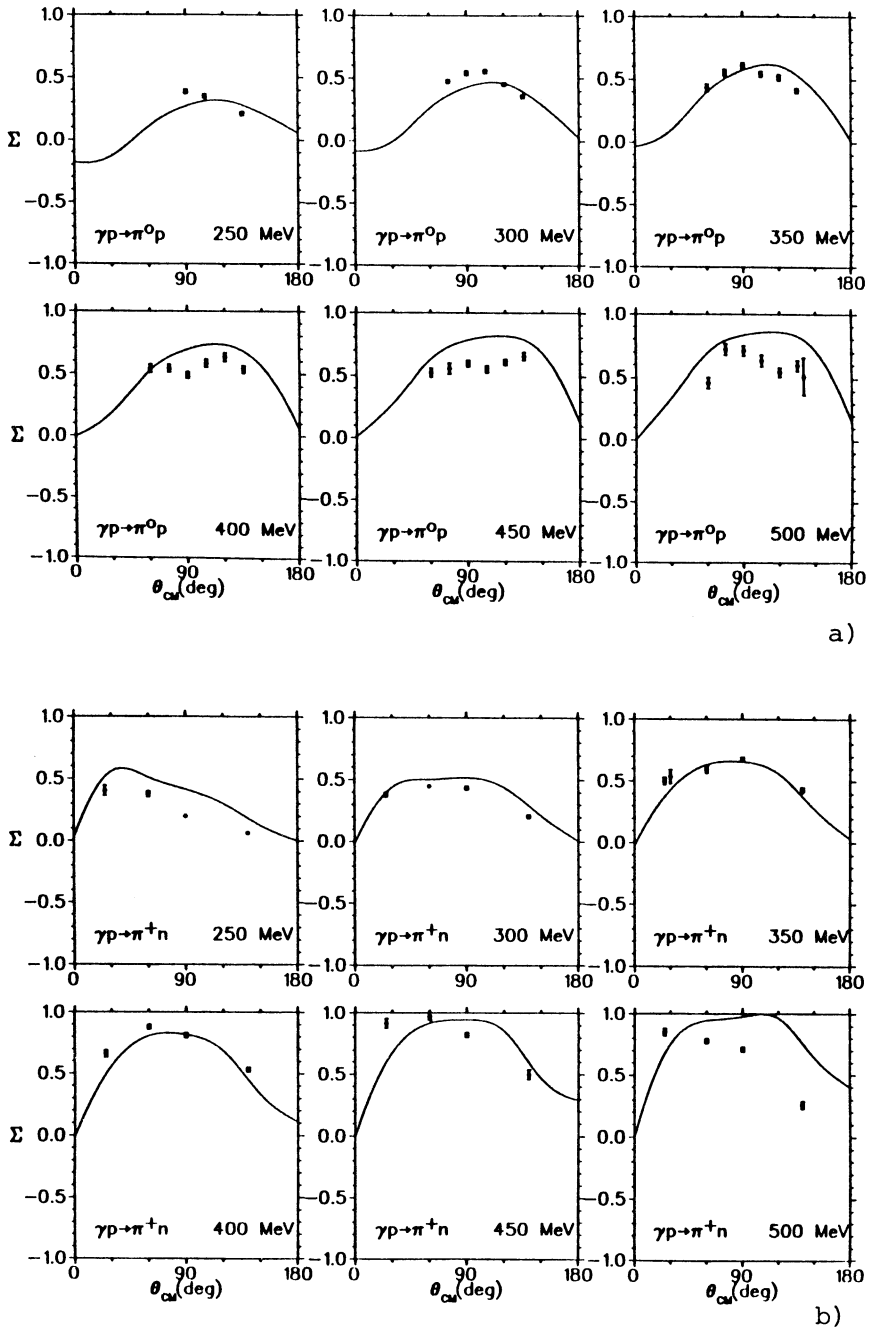
$\gamma p \to \pi^0 p$ 250 MeV
$\gamma p \to \pi^0 p$ 300 MeV
$\gamma p \to \pi^0 p$ 350 MeV
$\gamma p \to \pi^0 p$ 400 MeV
$\gamma p \to \pi^0 p$ 450 MeV
$\gamma p \to \pi^0 p$ 500 MeV
Σ
θ_{CM}(deg)
a)
$\gamma p \to \pi^+ n$ 250 MeV
$\gamma p \to \pi^+ n$ 300 MeV
$\gamma p \to \pi^+ n$ 350 MeV
$\gamma p \to \pi^+ n$ 400 MeV
$\gamma p \to \pi^+ n$ 450 MeV
$\gamma p \to \pi^+ n$ 500 MeV
b)

Fig. 16

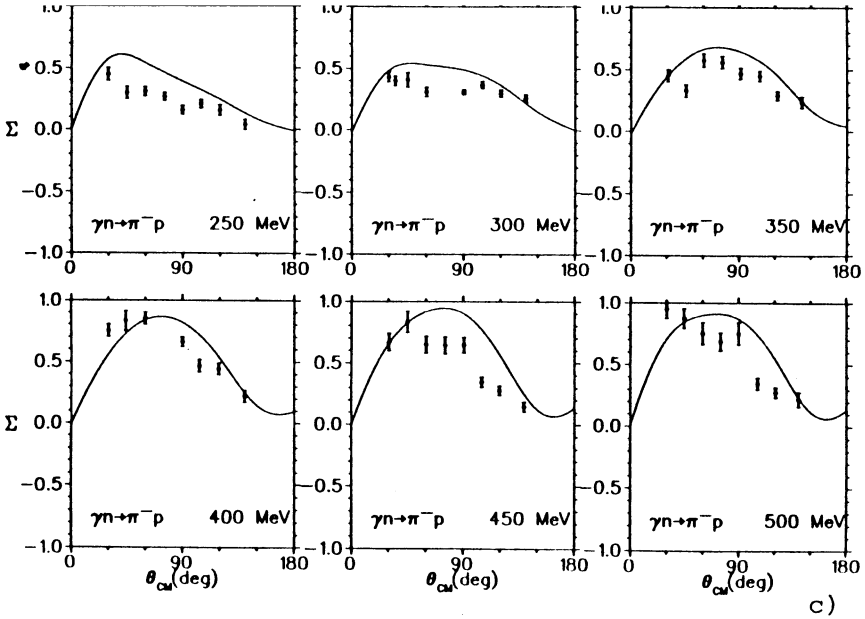
Σ
γn→π⁻p 250 MeV
γn→π⁻p 300 MeV
γn→π⁻p 350 MeV
γn→π⁻p 400 MeV
γn→π⁻p 450 MeV
γn→π⁻p 500 MeV
θ_CM (deg)
c)

Fig. 16

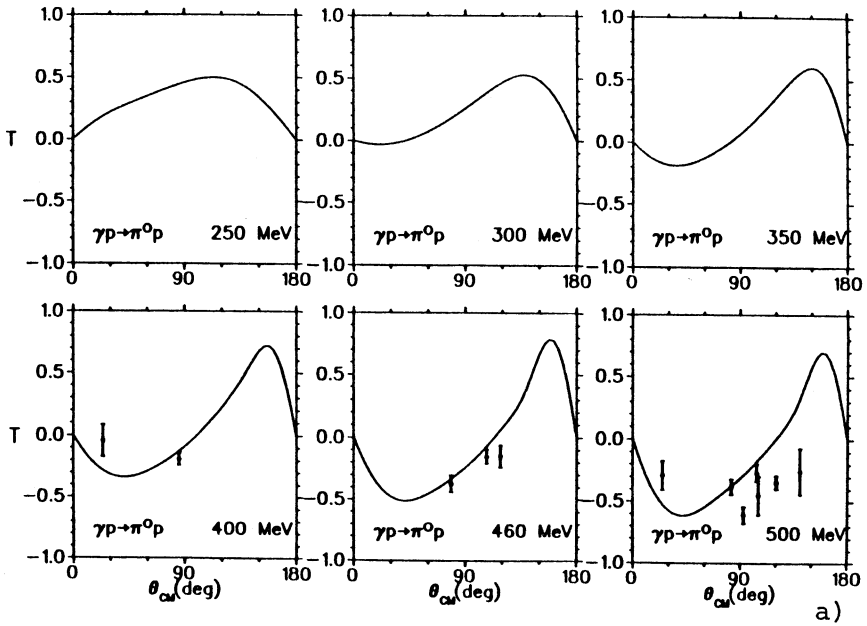
T
γp→π⁰p 250 MeV
γp→π⁰p 300 MeV
γp→π⁰p 350 MeV
γp→π⁰p 400 MeV
γp→π⁰p 460 MeV
γp→π⁰p 500 MeV
θ_CM (deg)
a)

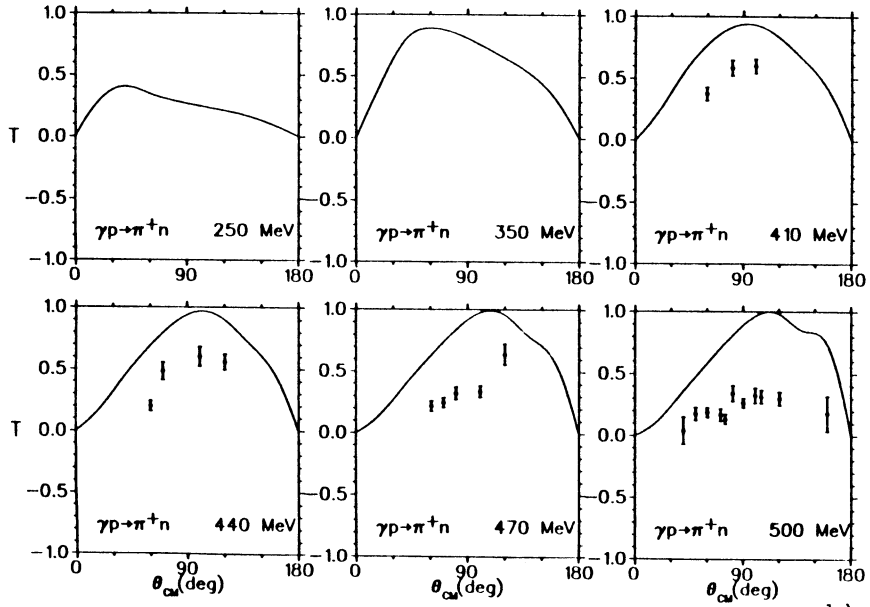
T
γp→π⁺n 250 MeV
γp→π⁺n 350 MeV
γp→π⁺n 410 MeV
γp→π⁺n 440 MeV
γp→π⁺n 470 MeV
γp→π⁺n 500 MeV
θ_CM (deg)
b)

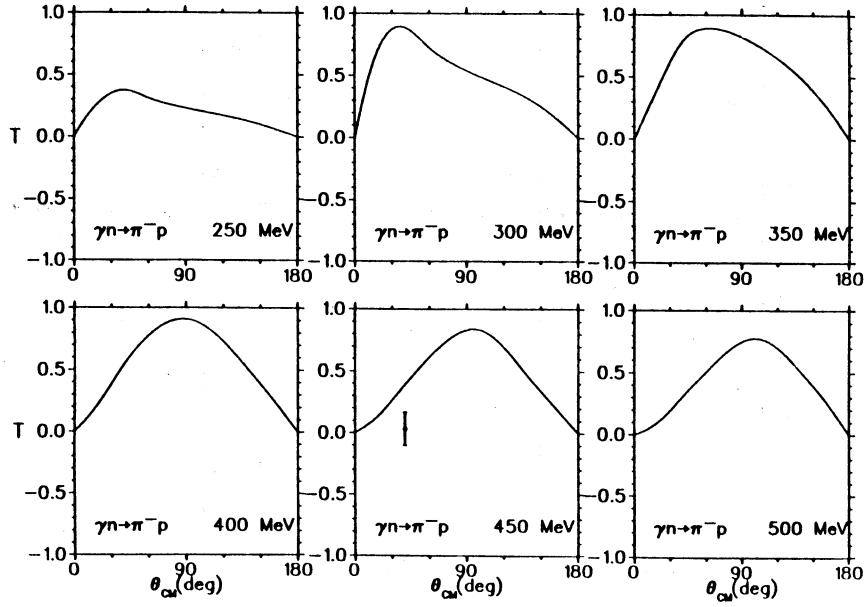
T
γn→π⁻p 250 MeV
γn→π⁻p 300 MeV
γn→π⁻p 350 MeV
γn→π⁻p 400 MeV
γn→π⁻p 450 MeV
γn→π⁻p 500 MeV
θ_CM (deg)
c)

Fig. 17

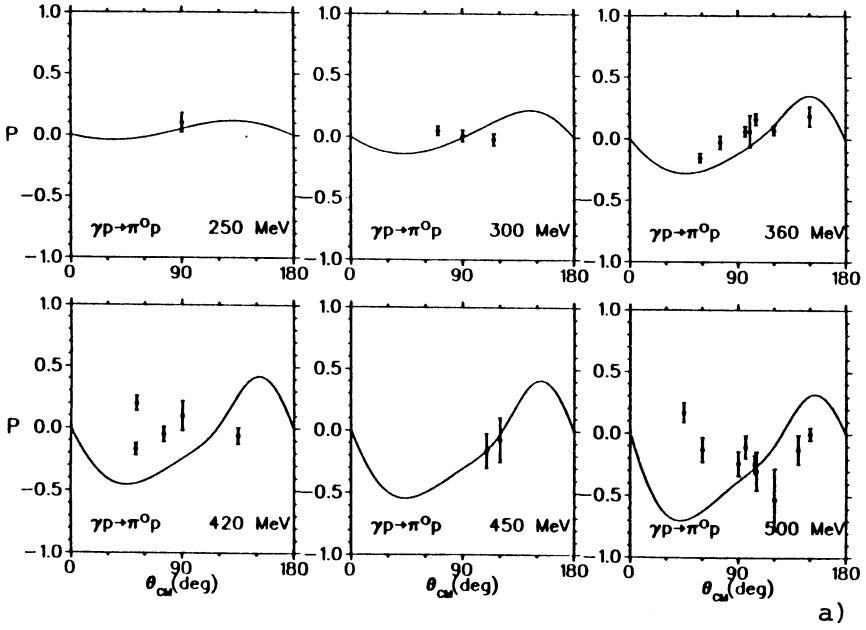
P
γp→π°p 250 MeV
γp→π°p 300 MeV
γp→π°p 360 MeV
γp→π°p 420 MeV
γp→π°p 450 MeV
γp→π°p 500 MeV
θ_CM (deg)
a)

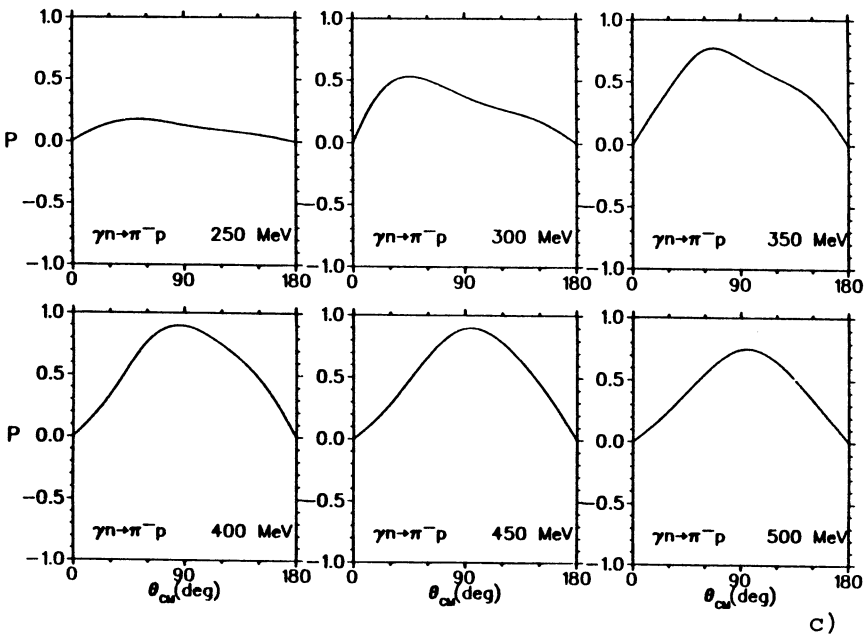
P
γn→π⁻p 250 MeV
γn→π⁻p 300 MeV
γn→π⁻p 350 MeV
γn→π⁻p 400 MeV
γn→π⁻p 450 MeV
γn→π⁻p 500 MeV
θ_CM (deg)
c)

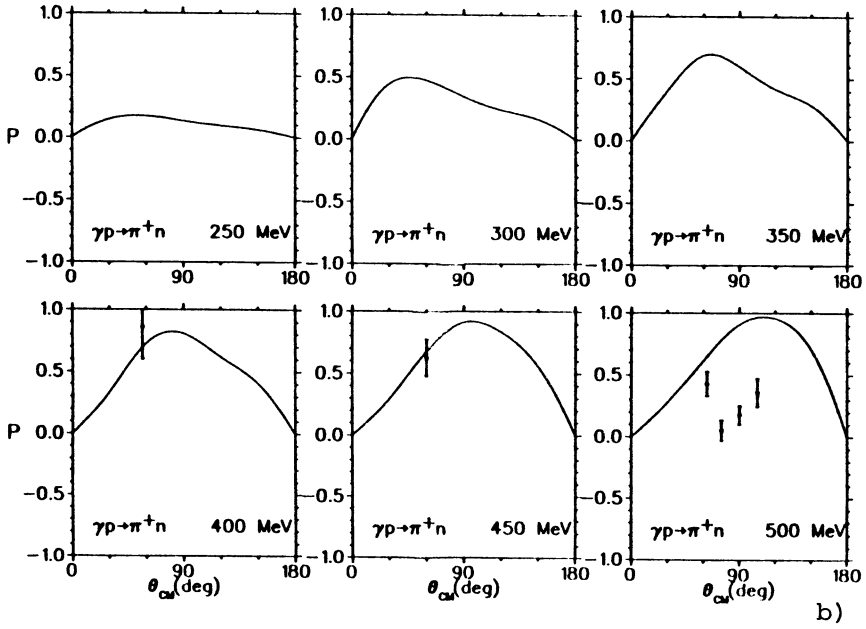
P
γp→π⁺n 250 MeV
γp→π⁺n 300 MeV
γp→π⁺n 350 MeV
γp→π⁺n 400 MeV
γp→π⁺n 450 MeV
γp→π⁺n 500 MeV
θ_CM (deg)
b)

Fig. 18